Technical Letter Report
TLR-RES/DE/CIB-2019-2

Assessment of the Continued Adequacy of Revision 2 of Regulatory Guide 1.99
Technical Letter Report

Dan Widrevitz
Matt Gordon

U.S. Nuclear Regulatory Commission
Office of Nuclear Regulatory Research

July 2019

DISCLAIMER:

This report was prepared as an account of work sponsored by an agency of the U.S. Government. Neither the U.S. Government, nor any agency thereof, nor any employee, makes any warranty, expressed or implied, or assumes any legal liability or responsibility for any third party's use, or the results of such use, of any information, apparatus, product, or process disclosed in this publication, or represents that its use by such third party complies with applicable law.

This report does not contain or imply legally binding requirements. Nor does this report establish or modify any regulatory guidance or positions of the U.S. Nuclear Regulatory Commission and is not binding on the Commission.

Table of Contents

List of Figures

List of Tables

List of Abbreviations

Abbreviation	Definition
¼-T	Location at one-quarter of the total thickness within the reactor pressure vessel as measured from the inner diameter
½-T	Location at half of the total thickness within the reactor pressure vessel as measured from the inner diameter
¾-T	Location at three-quarters of the total thickness within the reactor pressure vessel as measured from the inner diameter
ADAMS	Agencywide Documents Access and Management System
ASME	American Society of Mechanical Engineers
ASTM	American Society for Testing and Materials
BWR	Boiling Water Reactor
BWRVIP	Boiling Water Reactor Vessel and Internals Program (EPRI)
CF	Chemistry Factor
$CF_{defined}$	Chemistry Factor defined as “mean reality” in simulation
CF_{FIT}	Chemistry Factor refit to surveillance data
CF_{SIM}	Chemistry Factor simulated from sampling mean and standard deviation
CFR	Code of Federal Regulations
CMM	Correlation Monitor Material (also called a standard reference material)
EMA	Equivalent Margins Analysis
EOL	End of License
EPRI	Electric Power Research Institute
F	Forging
f_{surf}	Fluence at inner diameter of reactor pressure vessel
ID	Inner Diameter
ISP	Integrated Surveillance Program
LWR	Light Water Reactor
MD	Management Directive
MRP	Materials Reliability Program (EPRI)
MTR	Material Test Reactor
NDT	Nil-Ductility Temperature
NIIAR	Research Institute of Atomic Reactors (Russia)
NRC	Nuclear Regulatory Commission
NRR	Office of Nuclear Reactor Regulation
P	Plate
PSF	Pool Side Facility
PSSP	PWR Supplemental Surveillance Program
PWR	Pressurized Water Reactor
RAMA	Radiation Modeling Application (BWRVIP)
REAP	Reactor Embrittlement Archive Project
RG	Regulatory Guide
RPV	Reactor Pressure Vessel
RMSD	Root-Mean-Square Difference
ΔRT_{NDT}	Shift in reference temperature for a reactor vessel material measured at the 30-ft-lb energy level
SLR	Subsequent License Renewal
SMR	Small Modular Reactor
SRM	Standard Reference Material (also called a correlation monitor material)

σ	Standard Deviation
σ_{Δ}	Standard deviation of ΔT_{41J} measurement
T_0	Reference temperature characterizing the onset of cleavage cracking at elastic or elastic-plastic instabilities (or both)
ΔT_{41J}	Metric term for ΔRT_{NDT}
TTS	Transition Temperature Shift
U.S.	United States of America
USE	Upper Shelf Energy
$USE_{(I)}$	Upper Shelf Energy Irradiated
$USE_{(U)}$	Upper Shelf Energy Unirradiated
ΔUSE	Shift in Upper Shelf Energy
VVER	Water-Water Energetic Reactor (Soviet PWR design)
W	Weld

Executive Summary

Regulatory Guide 1.99, "*Radiation Embrittlement of Reactor Vessel Materials*," Revision 2 (RG1.99) describes methods that may be used to predict the effects of radiation embrittlement of reactor pressure vessels (RPV). Specifically, neutron irradiation of the RPV steel results in material property changes making the steel more brittle and potentially susceptible to rapid failure under high-stress conditions. This effect increases with neutron fluence (a measure of neutrons passing through a location or material). The embrittlement of RPV steels can pose a safety challenge and directly informs plant pressure-temperature limits. The most recent revision of this regulatory guide was published in 1988. It was expected, at the time of publication, that the regulatory guide would be updated and refined as more material data were collected.

The performance of this regulatory guide (RG) has proven sufficient such that no pressing need presented itself to update it for an extended period. This assessment was conducted as part of the regular reassessment of RGs. The purpose of this assessment was to determine the continuing adequacy of the RG under near- to mid-term conditions in the operating fleet and for new light water reactor builds.

The results of this assessment found deficiencies in nearly every aspect of the RG, with aspects of both safety significance and unjustified burden. Many of these deficiencies were identified as long-term problems during the last RG revision; new deficiencies were identified during this assessment. While the performance of RG is currently adequate for operating plants, all aspects of the RG merit further attention as fluence values increase, new material chemistries are used in new vessels, and new operating temperature regimes are proposed. For operating plants potentially experiencing higher fluence levels, these deficiencies could become a concern in the mid-2020s.

The RG includes guidance on five topics:

1) A formula to predict ΔT_{41J} (often referred to as ΔRT_{NDT})
2) A formula to predict ΔUSE
3) Methods to adjust ΔT_{41J} to take account of plant-specific surveillance data
4) Adjustments to ΔT_{41J} and ΔUSE to account for neutron attenuation through the RPV wall
5) Embrittlement limits for "new" plants.

This assessment provides results concerning the first four of these topics as well as several additional considerations that have become part of common practice in predicting the above, namely the degree-per-degree adjustment to account for irradiation temperature effects, and the use of sister-plant data. The embrittlement limits for "new" plants appear to have been based on supporting prior requirements in Appendix G of 10 CFR Part 50, which required that vessels be designed to permit a thermal annealing if the adjusted reference temperature exceeds 200°F during the RPV service life; this consideration is no longer pertinent because the Appendix G requirement has been eliminated.

The results of the assessment indicate that the predictions of both ΔT_{41J} and ΔUSE are inaccurate under many conditions. In the case of high neutron fluences, such as experienced by pressurized-water reactors in license renewal periods of extended operation, use of the RG may provide non-conservative results. Other sources of inaccuracy in the RG predictions lead

predominantly to unjustified burden, although the potential for non-conservative results for ΔUSE exists for a substantial portion (~19%) of materials.

The original RG acknowledged the potential for some of these inaccuracies and presented guidance for adjusting ΔT_{41J} and ΔUSE results based on future material surveillance data. Unfortunately, this guidance is deficient in several respects, including a higher probability of rejecting new data as credible as more data become available. The adjustment also inappropriately privileges the predictions of the RG trend curve even when high quality data may indicate otherwise. This privilege is problematic as the trend curve has significant residuals as noted above.

Regarding the attenuation adjustment, the formula provided in the RG has proven durable and accurate for regions of RPVs horizontally adjacent to the active fuel region. As the operating fleet ages, areas above and below the core are exceeding the threshold fluence where irradiation effects should be considered. The RG lacks any proper guidance (or cautions) regarding those areas.

Based on the results of the assessment, as summarized above, it is recommended that the RG be updated. It is also recommended that work to develop and finalize the RG update begin immediately to support implementation by the operating fleet in a timely fashion. Completion before the mid-2020s is recommended as high-fluence conditions will be reached during this period. Updated guidance will also benefit the design and operation of new reactors.

1. Introduction

Regulatory Guide (RG), 1.99, Rev. 2 (hereafter RG1.99), entitled "*Radiation Embrittlement of Reactor Vessel Materials,"* [RG1.99] describes methods acceptable to the NRC staff that may be used to account for the effects of radiation embrittlement on certain mechanical properties used to characterize the resistance of RPV steels to fracture. This report presents a summary of the results of assessing RG1.99.

This effort follows an assessment conducted in 2014 per Management Directive 6.6 [MD6.6]. The January 2014 assessment included a commitment "to complete a detailed evaluation of embrittlement prediction methodologies, data, and understandings to assess their impact on RG1.99 [and to] publish a report on this evaluation, including a determination of the future need to revise RG1.99, in approximately two years' time." Known limitations of RG1.99 have existed since its original publication and are described in part in the associated Regulatory Analysis [NRC 87],

> The proposed implementation of Revision 2 is final in the sense that there is no intent to return to Revision 1. There is, however, a strong probability that revisions will continue to be made over the lifetime of the plants as more data are added around the "fringes" of the data base: high nickel materials, low copper "modern" steels, and high fluence conditions encountered in plant life extension.

This assessment was conducted to verify the claims regarding the limitations of RG1.99, identify any new limitations, and present preliminary conclusions regarding the adequacy of RG1.99.

The contents of RG1.99 were based on "curve fitting" of surveillance data available in the mid-1980s a technique which is best suited to predictions within the data boundaries used to generate the curve fit (interpolation). In the case of RG1.99, the data used to generate its correlations, as noted in the Regulatory Analysis quoted above, were limited for certain parameters. These limitations are well defined in RG1.99.

The structure of the report is as follows:

Section 2	Assessment of the RG1.99 ΔT_{41J} trend curve
Section 3	Assessment of the RG1.99 ΔUSE trend curve
Section 4	Assessment of the RG1.99 credibility criteria and use of credible surveillance data
Section 5	Assessment of the RG1.99 attenuation formula
Section 6	Assessment of commonly used or discussed extensions to RG1.99; sister plant data and the degree-per-degree temperature adjustment
Section 7	Summary of preliminary findings regarding fleet impact

The discussion of fleet impacts distinguishes, where appropriate, between the operating fleet for which license renewal and subsequent license renewal is of primary interest and "new" reactors (post 2000 designs such as the AP-1000) that will be entering initial operation. This assessment endeavors to distinguish impacts that represent burden through overly conservative results or potential safety-consequence through insufficiently conservative (or insufficiently accurate) results.

2. RG1.99 ΔT41J Trend Curve

The RG1.99 ΔT_{41J} trend curve predicts radiation-induced embrittlement in RPV steels as a function of a chemistry factor and fluence at the location of interest via RG1.99 Eqs. 2 and 3. The chemistry factor is a function of weight-percent Cu and Ni. The chemistry factor is determined from RG1.99 Tables 1 and 2. Results concerning residuals, prediction error, and predictive accuracy relative to fluence, chemistry, etc. are presented. This analysis was conducted by partitioning measured data and evaluating RG1.99 ΔT_{41J} predictions against these partitions (base or weld material, pressurized-water reactor (PWR) or boiling-water reactor (BWR), etc.). Similarly, RG1.99 ΔT_{41J} predictions were analyzed to assess performance relative to input variables including those of RG1.99 and those found to have some impact on the performance based on the scientific literature.

Several results were expected prior to the conduct of this assessment. First, the fluence function *f* of RG1.99 becomes unsuitable at very high neutron fluence as illustrated in Figure 2-1. This function was not chosen to model embrittlement at very high fluence; rather, its performance was judged adequate for fluences below 1 x 10^{20} n/cm^2 (E > 1 MeV). Of the 177 data points used to generate the RG1.99 trend curve, the highest fluence data points were ~8 x 10^{19} n/cm^2 (E > 1MeV). Further investigation has not improved the expected accuracy of the fluence function, *f,* at high fluence. It is important to note that as the fluence function and chemistry factors were fit together, adjusting the fluence function independently of the chemistry factors does not eliminate the high fluence issue.

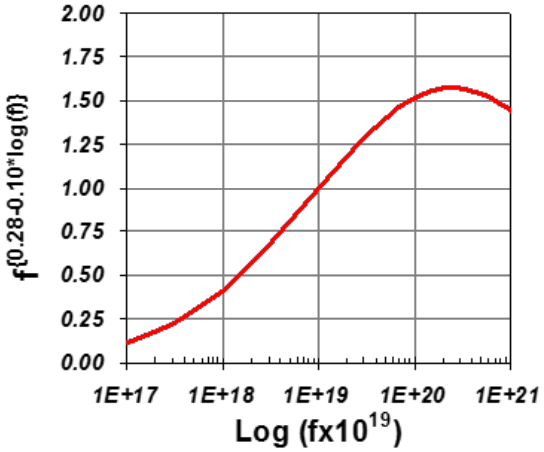

Figure 2-1. RG1.99 Fluence Function *f*

Consequently, the RG1.99 ΔT_{41J} (often denoted as ΔRT_{NDT}) trend curve should be expected to become increasingly inaccurate as fluence increases, eventually becoming invalid as fluence exceeds 10^{20} n/cm^2 (E > 1MeV).

Second, as the RG1.99 ΔT_{41J} was created as a curve fit, it is expected that its predictions will be most accurate for inputs within the bounds of the data used to fit the curve. Third, the ΔT_{41J} trend curve is stated as being valid between 274°C and 310°C (525°F and 590°F) without correction, although this was later supplemented by suggesting the degree-per-degree

adjustment[1]. The intent of this adjustment was to allow use of data from different plants with different operating temperatures. Finally, any phenomena that evolves with fluence in a manner unlike the function chosen for the trend curve may be poorly modeled. This assessment is designed to highlight the inherent strengths and weaknesses of the trend curve by comparing predicted values to measured values.

2.1 Data Used

The RG1.99 ΔT_{41J} trend curve was assessed using a subset of a recent data collection performed by American Society for Testing and Materials (ASTM) Subcommittee E10.02, "On Behavior and Use of Nuclear Structural Materials." The ASTM effort included the compilation and verification of ΔT_{41J} data and is discussed in detail in the ASTM E900 adjunct data-package [ADJE090015-EA]. The focus of the effort was restricted to mutually comparable steels used in light-water reactors (LWRs) of western design; thus, the ex-Soviet water-water energetic reactor (VVER) steels were not considered. The applicable data is summarized in Table 2-1. The original data set used to develop RG1.99 only had 177 data points versus the 1901 data points available for the assessment.

Table 2-1. Count of power reactor ΔT_{41J} records in the BASELINE in different categories of reactor type and product form.

Product Form	ΔT_{41J} Data	
	PWR	BWR
Weld	509	165
Plate	499	147
Forging	377	44
SRM*	153	7
Σ	1538	363

* Standard reference material

From these data, ASTM defined a BASELINE data subset for the purposes of ΔT_{41J} trend curve equation assessment. To be in the BASELINE subset, the steel had to be of commercial grade; have all descriptive variables known (i.e., copper, nickel, manganese, phosphorus, fluence, flux, temperature, and product form); have been exposed to neutron irradiation in a power reactor; and had embrittlement quantified by ΔT_{41J} measured using full-size Charpy V-notch specimens. The BASELINE subset included 1,878 ΔT_{41J} surveillance data from 13 countries: Belgium, Brazil, France, Germany, Holland, Italy, Japan, Mexico, South Korea, Sweden, Switzerland, Taiwan, and the United States. Of the 1901 records, 23 were not used due to missing one or more critical parameters needed for the assessment. No data from Material Test Reactor (MTR) sources were included. Figure 2-2 shows the division of the BASELINE data between these different countries with the U.S. data being the most predominant.

[1] Originally presented as "studies have shown that for temperatures near 550°F, a 1°F decrease in irradiation temperature will result in approximately a 1°F increase in [ΔT_{41J}]" [Wichman 1998]. More recently, Derbarberis, et. al., confirmed this result [Debarberis 2005]

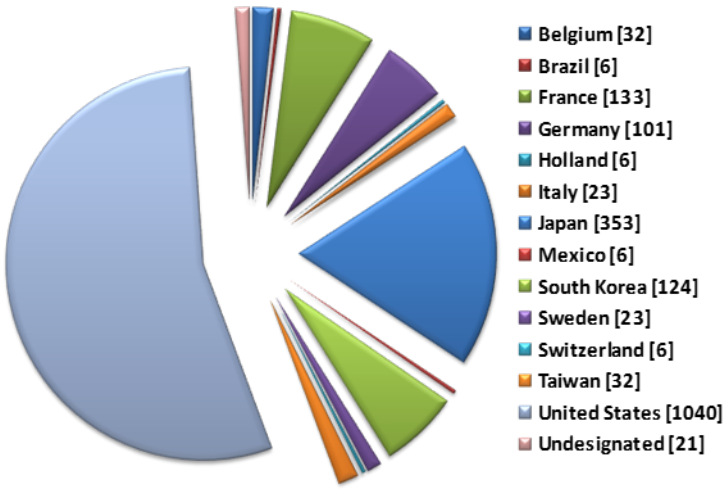

Figure 2-2. Distribution of PWR and BWR ΔT_{41J} surveillance data by nation of origin.

International data were used as part of this assessment to better assess the predictions of RG1.99 in areas where the U.S. data is sparser such as low Cu and/or high Ni (typical of newer reactors and future builds). The breadth of data used is illustrated in Figure 2-3.

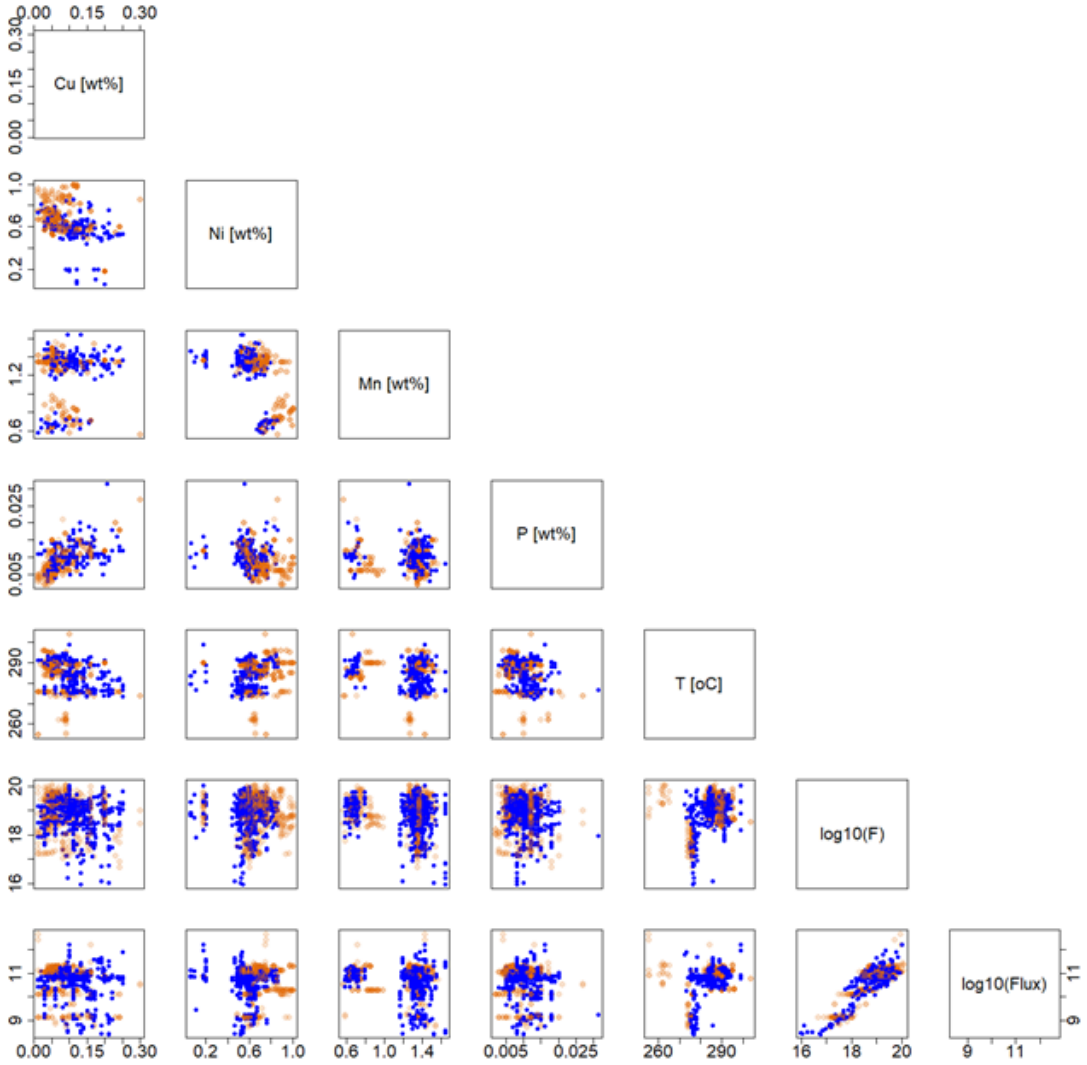

(a) Base Metals - Blue points are U.S. surveillance data, orange points are international surveillance data.

Figure 2 3. Distribution of variables important to the prediction of embrittlement trends. (a) Base metals and (b) weld metals.

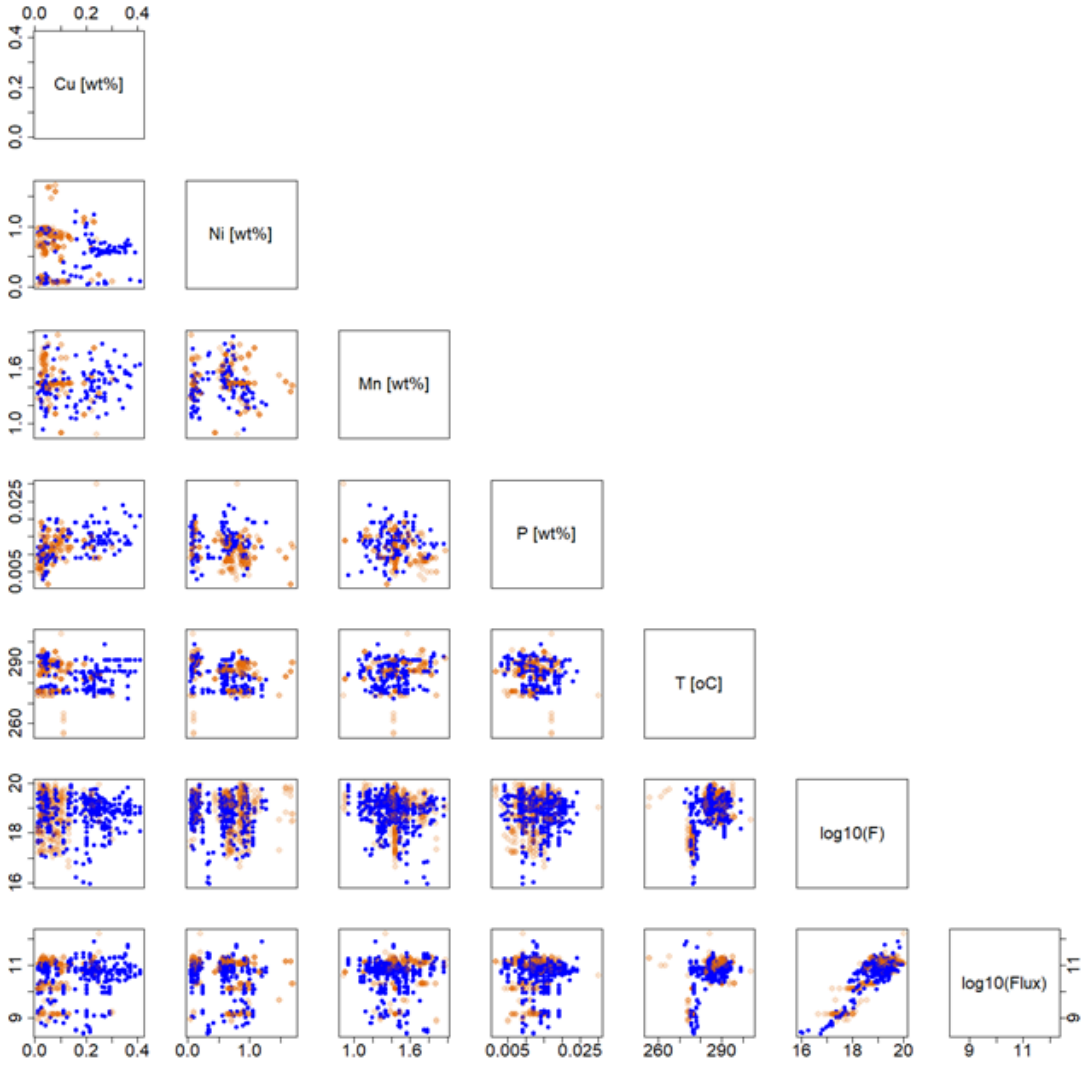

(b) Weld Metals - Blue points are U.S. surveillance data, orange points are international surveillance data.

Figure 2-3. Distribution of variables important to the prediction of embrittlement trends. (a) Base metals and (b) weld metals.

The international data also contains a higher percentage of high fluence data (fluence > $1x10^{19}$ n/cm^2, E > 1 MeV) that is of interest as it lies beyond the bulk of power reactor data used to fit the RG1.99 trend curve. Additional domestic U.S. data at high fluence is expected to become available from the present time through the 2020s (and beyond) via the coordinated reactor vessel surveillance and PWR supplemental surveillance program (PSSP) [Server 2017] and scheduled surveillance capsule withdrawals in U.S. plants. In addition, the international data includes values from Chooz-A (decommissioned in 1991), which were subjected to a much lower irradiation temperature (e.g., 255-265°C, 491-509°F, depending on material and record) than the range for the rest of the data. The Chooz-A results are of interest as its vessel irradiation temperature is similar to that of the proposed NuScale reactor design and is considerably lower than the other data (outside of the temperature zone of stated applicability of RG1.99).

2.2 **Bias and Uncertainty**

The bias and uncertainty assessment results for RG1.99 are shown in Figure 2-4. Results are shown with and without a degree-per-degree adjustment. This adjustment was discussed in a NRC staff presentation authored by Wichman [Wichman 1998]. The Wichman presentation states that studies had observed that, for irradiation temperatures near 288°C (550°F) an additional degree of ΔT_{41J} shift occurred per degree of irradiation temperature below 288°C (550°F); the converse holds for irradiation temperature above 288°C (550°F). In other words, operation at 287°C would give a ΔT41J shift that is 1°C higher than that at 288°C; operation at 549°F is thought to give a ΔT41J shift that is 1°F higher than that at 550°F. This adjustment is not accounted for in the RG1.99 trend curve.

The top plots of Figure 2-4 illustrate the magnitude of the mean residual. The mean residual indicates the average deviation between all predicted results and corresponding measurements. A positive value indicates that the predicted values are higher than the measured values. A negative value indicates that the predicted values are lower than the measured values. This is a direct indication of the accuracy, or bias, of RG1.99 relative to measured ΔT_{41J}.

The predictions of RG1.99 produce generally positive bias of 3-7°C (5-13°F) in relation to the U.S. data (central column of Figure 2-4); this effect is increased if the degree-per-degree adjustment is made. This positive bias is a conservative trend as it results in over-prediction of embrittlement.

The middle plots of Figure 2-4 illustrate the magnitude of the root-mean-square difference (RMSD). The RMSD statistic demonstrates a measure of the average deviation (positive or negative) of the predictions versus measurements. The higher the RMSD value, the larger the average individual deviations are between predicted and measured values. This is a measure of the uncertainty of RG1.99 relative to ΔT_{41J}. Results with high RMSD may have zero bias but they have poor precision due to many high deviation data that average each other out. RMSD is analogous, and under certain conditions identical, to standard deviation.

The RMSD for the U.S data in Figure 2-4, 14 and 19°C (25 and 34°F) for base and weld material respectively, is higher than the RG1.99 standard deviation values of 9.4°C and 15.6°C (17 and 28°F) for base and weld material respectively. The RMSD results for international data are considerably worse. The degree-per-degree adjustment makes little change in RMSD value.

The bottom plots of Figure 2-4 illustrate the magnitude of the log(likelihood) of the predictions. This measure gives insight into the likelihood that a given dataset would be produced by an assumed relationship. In this case, greater values (closer to 0) indicate a higher likelihood that the measured results match the predicted RG1.99 relationship. Likelihood is a common measure used to fit functions to data through maximization routines. The log(likelihood) results indicate that the RG1.99 trend curve has the greatest residuals for base metals, PWRs, high Ni, and high Cu (for U.S.). Application of the degree-per-degree adjustment worsened residual results as measured through log(likelihood) particularly for base metal, PWR, and low Cu materials.

The log(likelihood) of RG1.99 with the degree-per-degree adjustment is worse when considering international data primarily due to Chooz-A data, which RG1.99 was not designed to predict (due to its low irradiation temperature. The effect of the degree-per-degree adjustment generally decreases the log(likelihood) results. This is consistent with the U.S. only results as

the degree-per-degree adjustment using RG1.99 leads to poorer results for the PWR and Low Cu data. It is likely that use of the degree-per-degree adjustment becomes more inaccurate as one moves away from 288°C (550°) and/or is too simple to fully account for a spectrum of Cu and temperature variances.

2.3 **Residual Trends**

The residuals assessment results for RG1.99 ΔT_{41J} relative to several input variables are shown in Figure 2-5. The Student's T-test values are plotted in the figure to illustrate residual trends relative to each of the indicated inputs. The lower the Student's T-test value, the more likely that the RG1.99 model accurately predicts the embrittlement trend relative to that input. For Student's T-tests, a value of 1.96 indicates that 95 percent of the data falls within 1.96 standard deviations of the mean, which is conventionally considered an acceptable fit. For example, the RG1.99 trend curve has no temperature term, a known simplification, consequently the T-test value for temperature is high. Adding the degree-per-degree adjustment to RG1.99 ΔT_{41J} significantly reduced (improved) the T-test results shown in Figure 2-5 for temperature. The outliers from Chooz-A data with regards to temperature does not strongly influence the T-test results illustrating a limitation of the T-test in that it is less sensitive to small but strong outlier signals.

The RG1.99 trend curve when analyzed using only U.S. data shows low residuals relative to Ni, P, and Mn. When the degree-per-degree adjustment is added, the residuals generally fall, although the residuals for Cu and Ni rise. The RG1.99 trend curve applied to international data shows high residuals for fluence/flux, Ni, temperature, and P. Adding the degree-per-degree adjustment to the international data results in high residuals for fluence/flux effects. Analyzing the RG1.99 with a combined U.S. and international dataset increases the residual signal for temperature especially, which is suppressed when the degree-per-degree adjustment is added, although this increases the residual results for Cu and flux/fluence.

The narrower sub-bins illustrated in Figure 2-5 (such as Base, Welds, BWRs, etc.) reveal that the aggregate residual results mask subtleties within the overall data-set. For example, the residuals for fluence/flux are larger for PWR than for BWR when considering only international data. This is likely due to the clustered nature of U.S. data relative to fluence/flux used to originally fit RG1.99, creating an "overfit" or lacking the mathematical terms to better reflect embrittlement over a broader range of fluence/flux. It is important to note here that fluence/flux and temperature are highly correlated in the U.S. data. Trends in the residual values relative to fluence/flux may, in fact, be due to temperature effects in RG1.99. This seems likely as the degree-per-degree adjustment decreases the fluence/flux residuals for U.S. data implying a relationship between these two inputs. Conversely the degree-per-degree adjustment increases the residuals for international data providing further support for an unmodeled effect in RG1.99. Consistent with the log(likelihood) results, the application of the degree-per-degree adjustment shows a variation in residual response when comparing low-Cu to high-Cu binning as well.

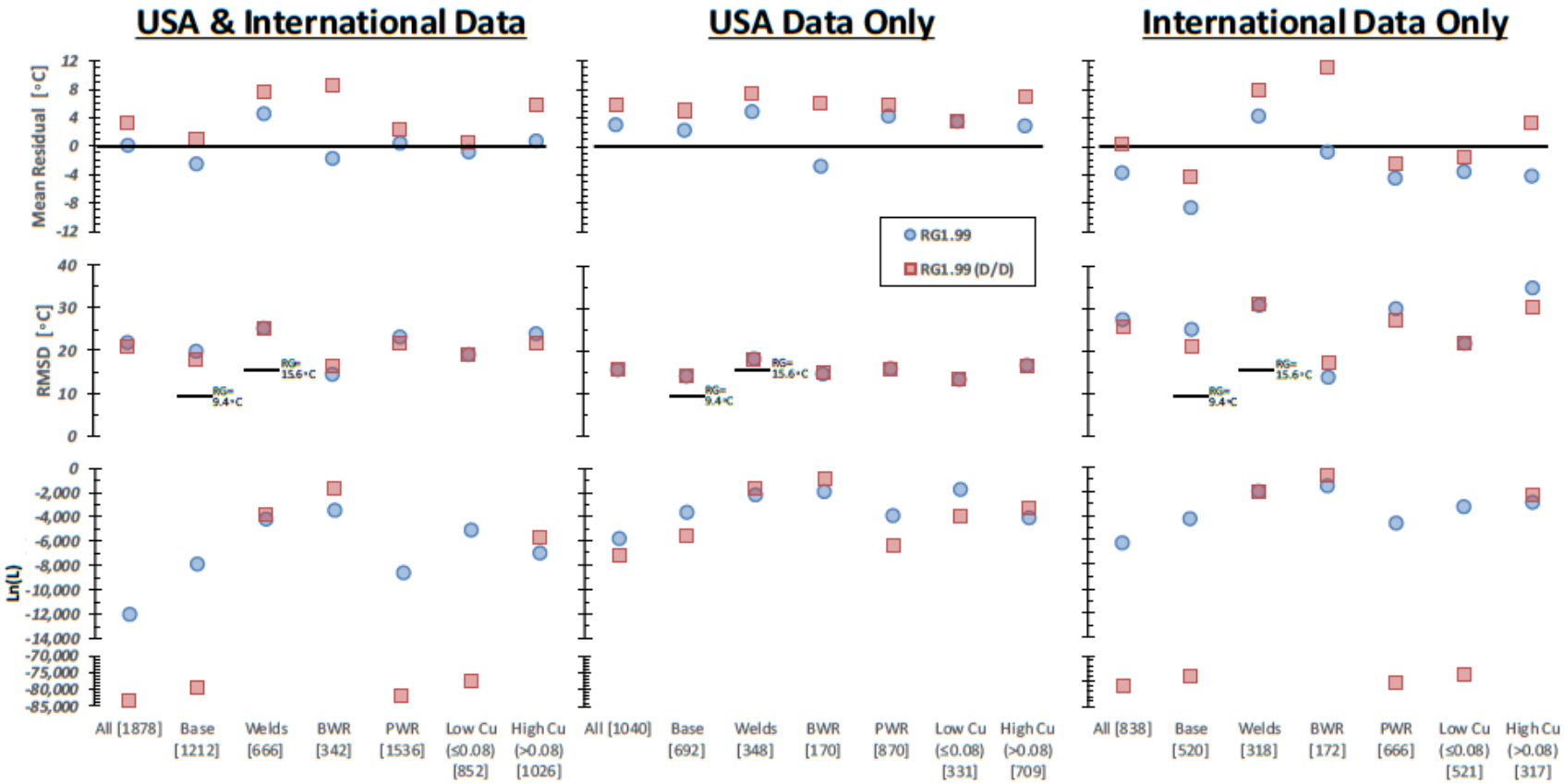

Figure 2-4. Values of mean residual (upper graphs), root-mean square deviation (middle graphs), and log(likelihood) (lower graphs) calculated for RG1.99, eq. (2-1) and RG1.99 degree-per-degree, eq. (4-2) trend curve predictions using different data partitions.

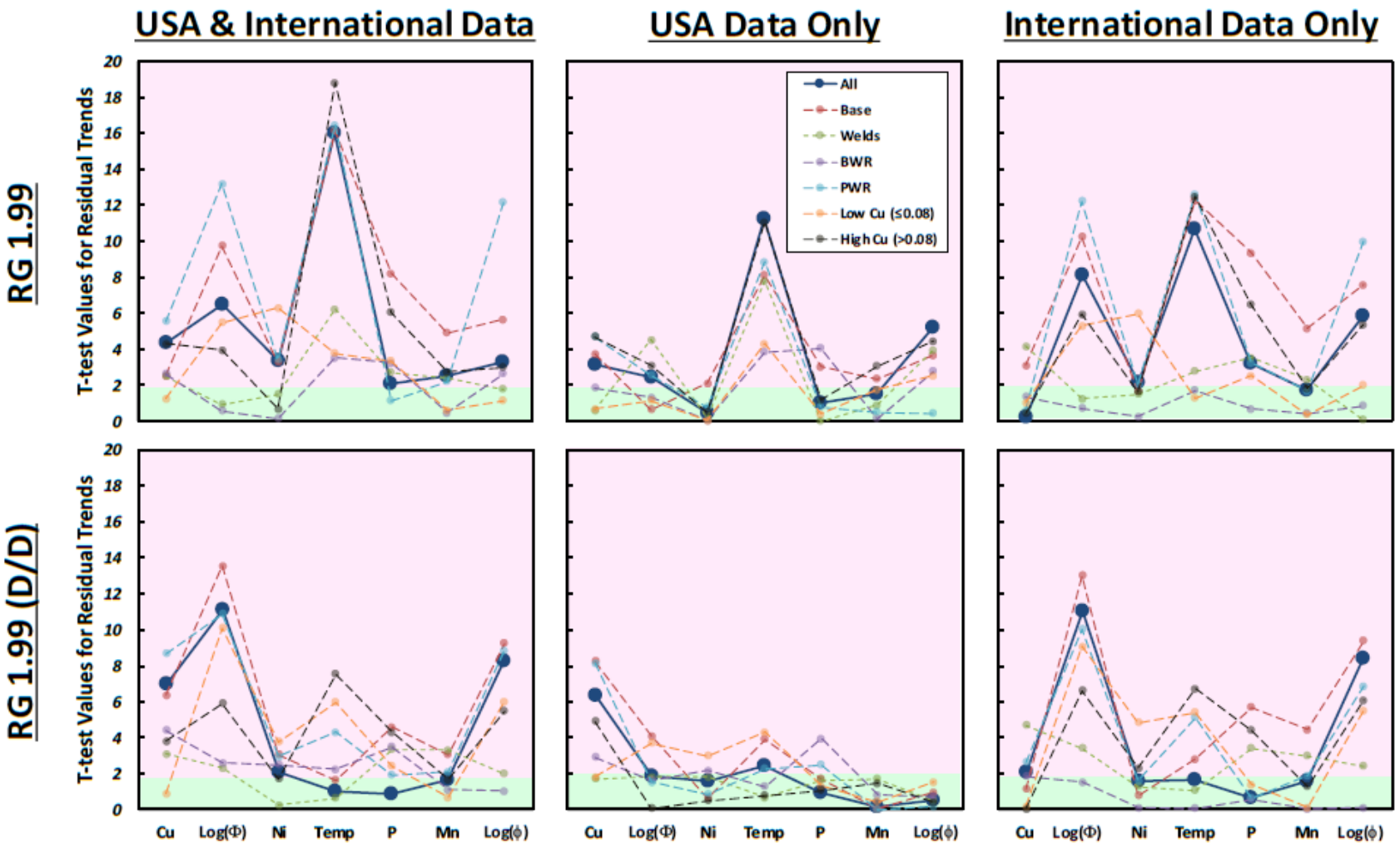

Figure 2-5. T-test values to assess residual trends relative to different regressor values and data partitions for RG1.99 ΔT_{41J}, and RG1.99 ΔT_{41J} with degree-per-degree, (upper and lower graphs, respectively). Red shaded regions indicate statistically significant residual trends. Here Φ denotes fluence and ϕ flux.

2.4 **Fleet Impact**

The assessment of RG1.99 prediction of ΔT_{41J} can impact the fleet in two ways. Predictions that are too high may cause burden by narrowing the operating window of pressure-temperature limits or increasing the required hydrostatic testing temperature. More importantly, predictions that are too low may lead to operation below required safety margins. To consider the fleet impact, the fluences associated with the original licenses and potential license extensions were estimated. Comparing this information to the difference between the predicted and measured values of RG1.99 ΔT_{41J} provides insight into the predictive limitations of RG1.99.

Results are shown in Figure 2-6. The fluences for each plant were estimated using information from MRP-326, "Coordinated PWR Reactor Surveillance Program," [MRP326] and BWRVIP-86 Rev. 1-A, "Updated BWR Integrated Surveillance (ISP) Program Implementation Plan [NP - ML13176A097]" [BWRVIP-86 1A]. As these results compare estimated fluences to measured values, they are approximate and should not be taken to reflect a fully accurate illustration of operating plant licensing bases.

Several trends are apparent. First, the estimates of embrittlement provided by RG1.99 appear to become non-conservative at fluence levels approaching 3 to 6 x 10^{19} n/cm^2 (E > 1 MeV). This is evident from the U.S. data and corroborated by the international data for base metals. The information is too sparse for weld metals to draw a similar conclusion. This is not solely due to the RG1.99 fluence function, *f,* as shown in Figure 2-1, but the fluence function is a contributor to this effect.

Second, a significant amount of data, U.S. and international, fall outside of the two-sigma standard deviation bounds illustrated in Figure 2-6. This is consistent with the results shown in Figure 2-4 indicating that the prescribed standard deviation in RG1.99 is lower than the standard deviation of the ASTM data set. Consequently, use of RG1.99 constitutes a less accurate prediction than is indicated in the guidance.

Finally, a slight bias exists in the RG1.99 prediction towards a conservative estimation of ΔT_{41J}, mostly at lower fluences; a trend visible as a slight upward bowing of the residual data from zero in Figure 2-6 before the data trends downwards. This too is consistent with the results shown in Figure 2-4 that indicate, particularly for the U.S. data, a positive overall bias in predictions.

The potential for underpredicting ΔT_{41J} is of interest to the safe operation of plants. As fluence increases, the potential to underpredict ΔT_{41J} increases. To provide some insight, Table 2-2 contains estimates of how many plants will achieve either 3 x 10^{19} n/cm^2 or 6 x 10^{19} n/cm^2 (E > 1MeV) for their limiting material relative to the original period of licensed operation and for potential license renewal operating periods. Based on this table, it is evident that a fluence limit should be established to indicate when RG1.99 ceases to adequately predict ΔT_{41J} for regulatory purposes.

Table 2-2. Estimated number of total licensed reactors above stated fluence organized by license period

Total Number of Reactors > 3x10^{19} n/cm^2			**Total Number of Reactors > 6x10^{19} n/cm^2**		
40 Year	60 Year	80 Year	40 Year	60 Year	80 Year
19	41	55	0	5	22

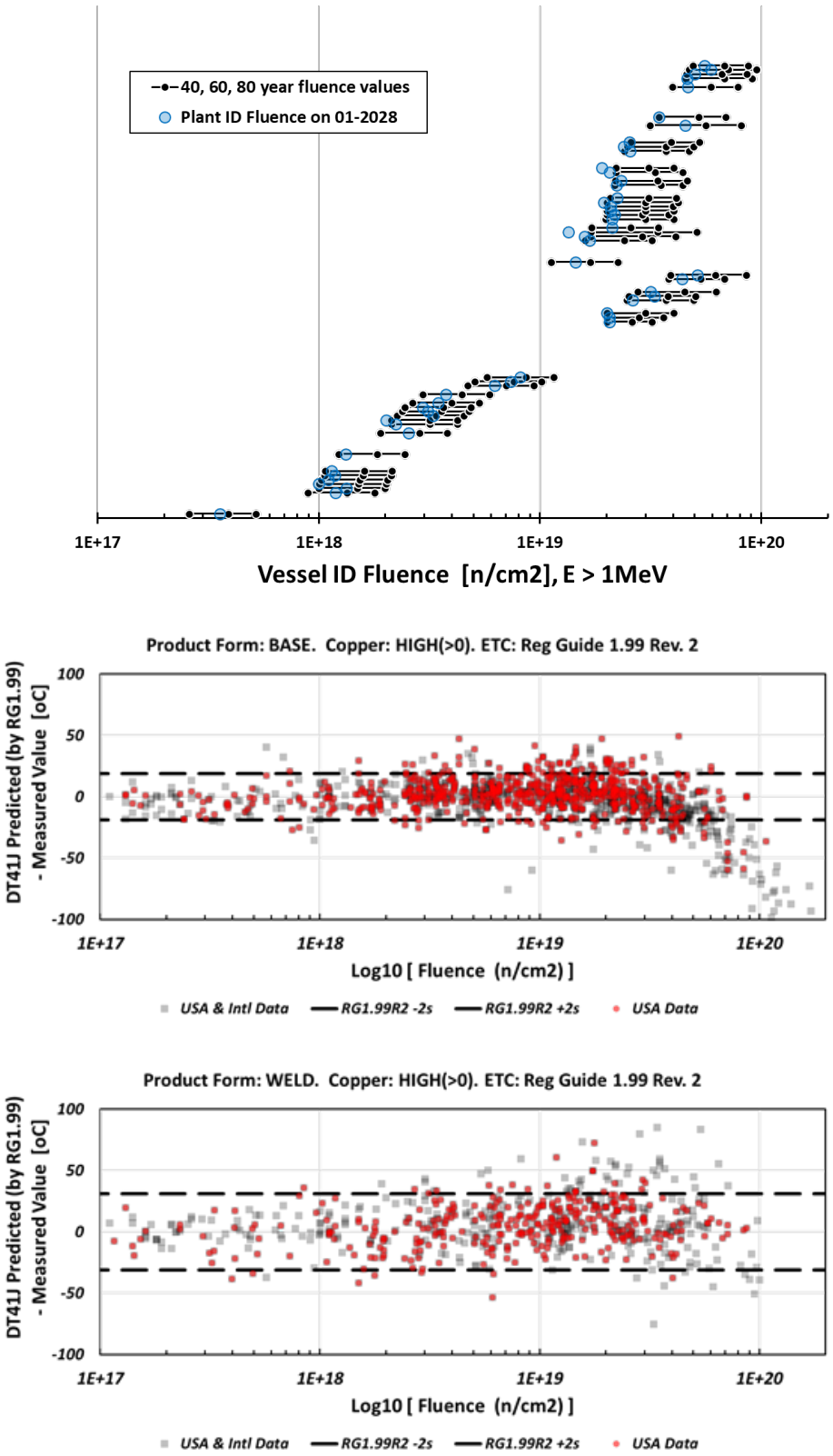

Figure 2-6. Fleet Impact Results. Top – Plant fluences; Middle – Delta ΔT_{41J} for Base Metals; Bottom – Delta ΔT_{41J} for Weld Metals. Two standard deviations plotted from RG1.99 values.

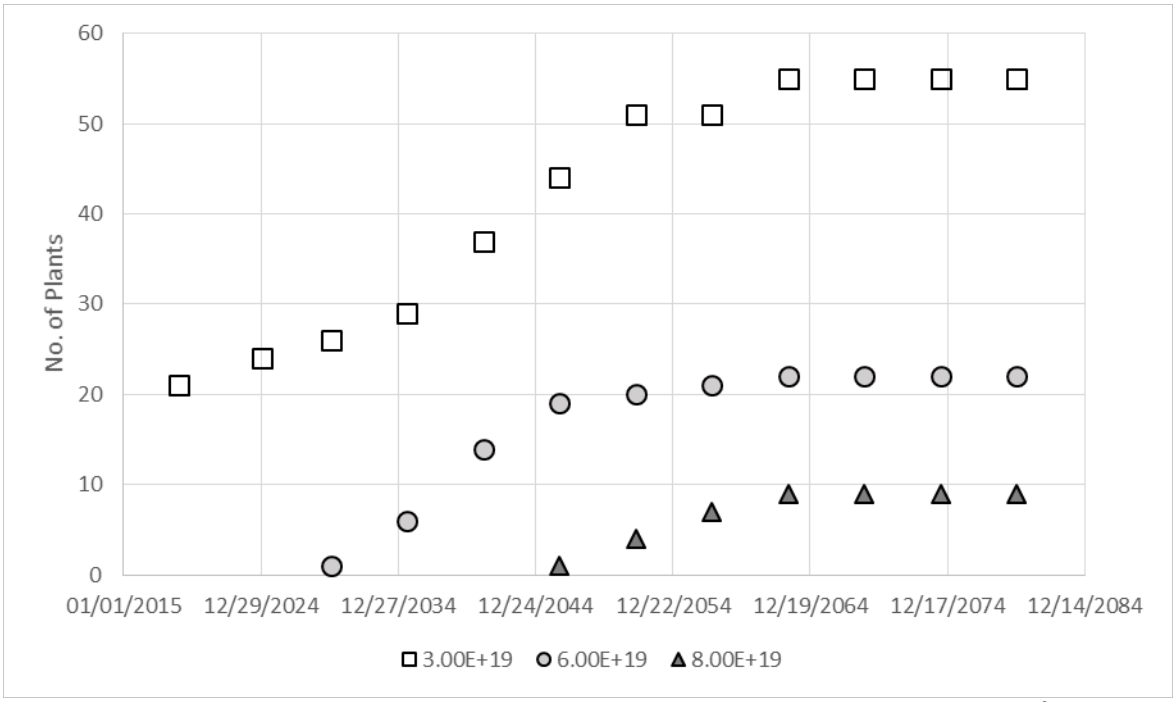

Figure 2-7. Number of reactors with maximum ID fluence exceeding specified fluence (n/cm^2, E > 1 MeV) values by year; assuming no new retirements.

Several operating reactors have already surpassed 3 x 10^{19} n/cm^2 (E > 1MeV). The first reactor to surpass 6 x 10^{19} n/cm^2 (E > 1MeV) will not do so until roughly 2028, within its first license renewal period. The second reactor to surpass this fluence would do so in 2033, also within its first license renewal period. The number of reactors with ID fluences meeting or exceeding 3 x 10^{19}, 6 x 10^{19}, or 8 x 10^{19} n/cm^2 (E > 1 MeV) is illustrated in Figure 2-7 plotted against calendar year. The plants with inner diameter (ID) fluences in the range of interest increase between 2020 and 2040 indicating that any modification of the trend curve relative to fluence would be of increasing importance as plants age within this time period. As this assessment was conducted by using estimated fluence trends, further attention may be warranted to affirm the accuracy of these dates.

The adverse results documented above, for low Cu materials, in particular, will likely reduce the accuracy of RG1.99 predictions for new reactors. Because new reactors are being designed with superior initial properties, the safety significance of inaccurate embrittlement prediction is less probable. Specifically, the recognition that copper content is detrimental to radiation embrittlement has been well communicated. The likelihood of adverse impact from the predictive inaccuracies of RG1.99 in a safety significant manner is low. While it is possible that RG1.99 under-predicts embrittlement for low Cu materials, the ultimate embrittlement of new reactor materials is likely to be low enough that this will not result in operating unsafely.

2.5 **Summary**

The assessment of the RG1.99 ΔT_{41J} trend curve indicates that several limitations exist that may have safety implications. First, the trend curve has significant bias, uncertainty, and likelihood issues that impact its predictive capacity for the operating fleet. This is particularly true at high fluence where the RG1.99 fluence function, *f,* ceases to match observed data in a non-conservative fashion. For new reactors, weaknesses in the RG1.99 trend curve are more

pronounced as new reactors have low Cu and at least one new reactor design has a notably low irradiation temperature that RG1.99 was not designed to accurately predict.

This assessment does not address actual licensing bases. Not all plants use the RG1.99 ΔT_{41J} trend curve directly as many supplement it with surveillance data or other adjustments such as degree-per-degree. For these plants, deficiencies in the trend curve are not expected to correlate directly to potential deficiencies in licensing bases. However, the trend curve inaccuracies are likely to create burden through interaction with the credible surveillance data use recommendations in RG1.99 that presuppose the superior accuracy of the RG1.99 model.

3. RG1.99 ΔUSE Trend Curve

The RG1.99 ΔUSE trend curves are given as Fig. 2 of RG1.99 and have no mathematical representation within the RG. The text indicates that linear interpolation is acceptable and that the trends are only valid between 274°C and 310°C (525°F and 590°F) and between the listed Cu and Ni contents. Use of the trends beyond this temperature range or the listed chemistries requires justification based on submittal of data. Results concerning residuals, prediction error, and predictive accuracy relative to fluence, chemistry, etc. are presented herein. To assess the ΔUSE predictions, the following mathematical approximations were used from RG1.162, "Format and Content of Report for Thermal Annealing of Reactor Pressure Vessel" [RG1.162]:

$$USE_{(I)} = USE_{(U)} \times \left(1 - \frac{D}{100}\right) \quad (3\text{-}1)$$

$$D = (100Cu + 9f)f^{0.2368} \text{ for base metals} \quad (3\text{-}2)$$

$$D = (100Cu + 14f)f^{0.2368} \text{ for weld metals} \quad (3\text{-}3)$$

Subject to the constraint that D never exceeds D_{MAX}:

$$D_{MAX} = 42.93f^{0.1502} \quad (3\text{-}4)$$

Here $USE_{(U)}$ denotes unirradiated values, while $USE_{(I)}$ denotes irradiated values; Cu is in weight percent and *f* is fluence in n/cm^2 (E > 1 MeV) divided by 10^{19}. The quantities $USE_{\%drop}$ and ΔUSE can then be calculated from this information using Eqs. (3-5) and (3-6), respectively:

$$\Delta USE \equiv USE_{(U)} - USE_{(I)} \quad (3\text{-}5)$$

$$USE_{(I)\%DROP} \equiv \frac{\Delta USE}{USE_{(U)}} * 100\% \quad (3\text{-}6)$$

3.1 **Data Used**

Surveillance information stored in the Reactor Embrittlement Archive Project (REAP) database was used to estimate $USE_{(U)}$ and $USE_{(I)}$ values. This information was merged, where possible, with the up-to-date information on composition and fluence from the American Society of Testing and Materials (ASTM) database, described in Section 2.1. This merged dataset combined measured unirradiated and irradiated ΔUSE results with updated chemistry and fluence values for each material. In addition, information on $USE_{(U)}$ and $USE_{(I)}$ for German PWRs, previously provided by AREVA to ASTM E10.02, was used as well.

$USE_{(U)}$ and $USE_{(I)}$ values were estimated from Charpy absorbed energy data using the procedure of ASTM E185, which is to average all energy values associated with specimens exhibiting 95% shear fracture area or greater [ASTM E185-82]. The U.S. and international data are presented in Figure 3-1 illustrating the breadth of the dataset. A more detailed breakdown of the data is shown in Table 3-1.

Table 3-1. Counts of USE(U) and USE(I) observations in different partitions.

	U.S. & International Surveillance	Just U.S. Surveillance	Just International Surveillance
All	1,223	1,016	207
Weld	399	329	70
Base	824	687	137
PWR	1,068	861	207
BWR	155	155	0
Low Cu (≤ 0.08)	495	328	167
High Cu (> 0.08)	728	688	40

3.2 Bias and Uncertainty

The bias and uncertainty assessment results for RG1.99 are shown in Figure 3-2 and are structured similarly to those shown for ΔT_{41J}. The mean and RMSD results suggest a consistent positive (conservative) bias and scatter in RG1.99 predictions. This trend is expected as RG1.99 predictions of ΔUSE were designed to be more bounding than "best estimate" and do not require additional standard deviation margin or plant-specific data adjustment. The large uncertainty indicated by the RMSD likewise is also expected as USE measurements have relatively high inherent scatter.

3.3 Residual Trends

The residuals assessment results for RG1.99 ΔUSE relative to several input variables are shown in Figure 3-3 and are structured similarly to those shown for ΔT_{41J}. The residual trends here are more difficult to interpret than for ΔT_{41J} because the ΔUSE results were designed to have inherent positive bias (i.e. conservatism). Nonetheless, significant residuals exist for most input variables shown, implying that the prediction is not incorporating significant behavior inherent in the data.

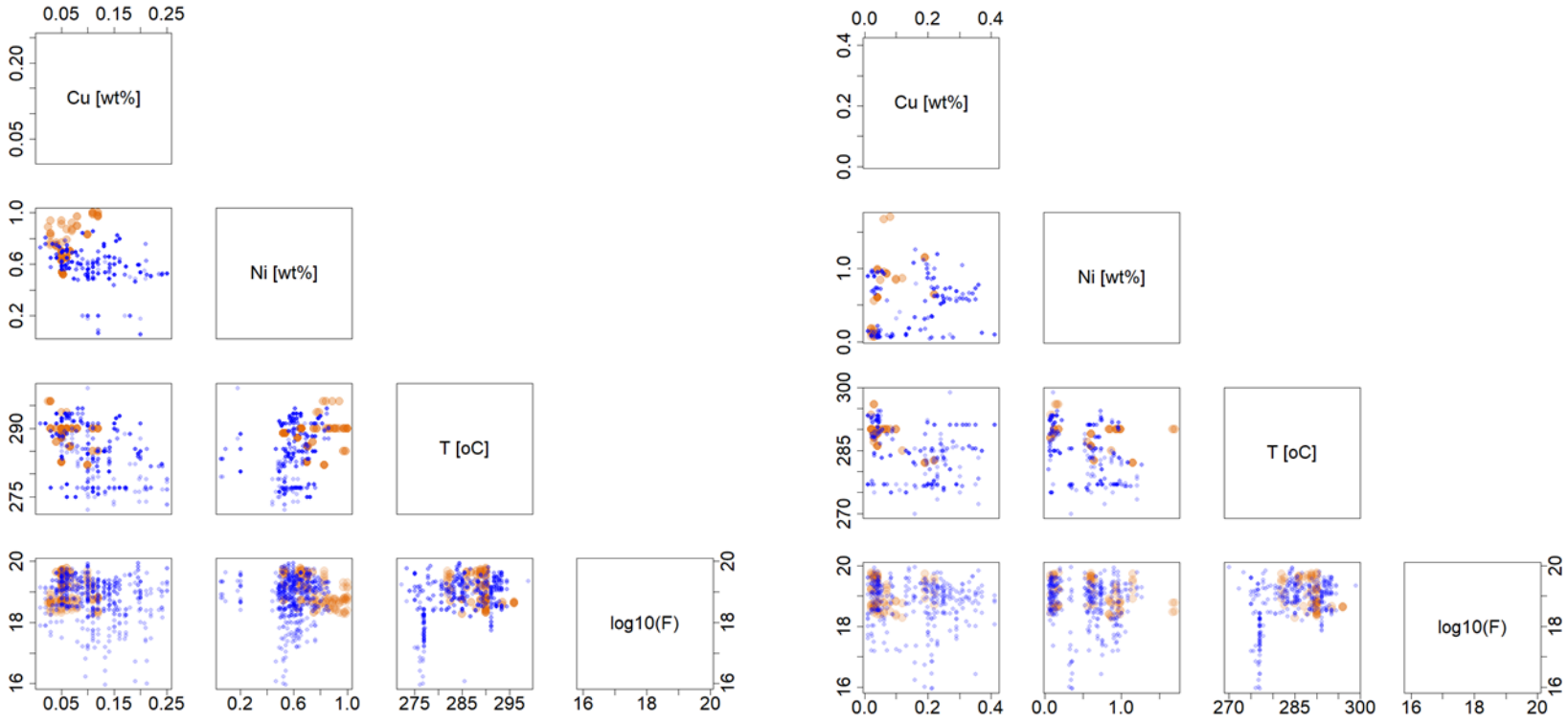

Figure 3-1. Plots showing the four key variables influencing embrittlement from the database used to evaluate USE. Left graphic: base metals, Right graphic: weld metals. U.S. surveillance data (blue points), International surveillance data (orange points).

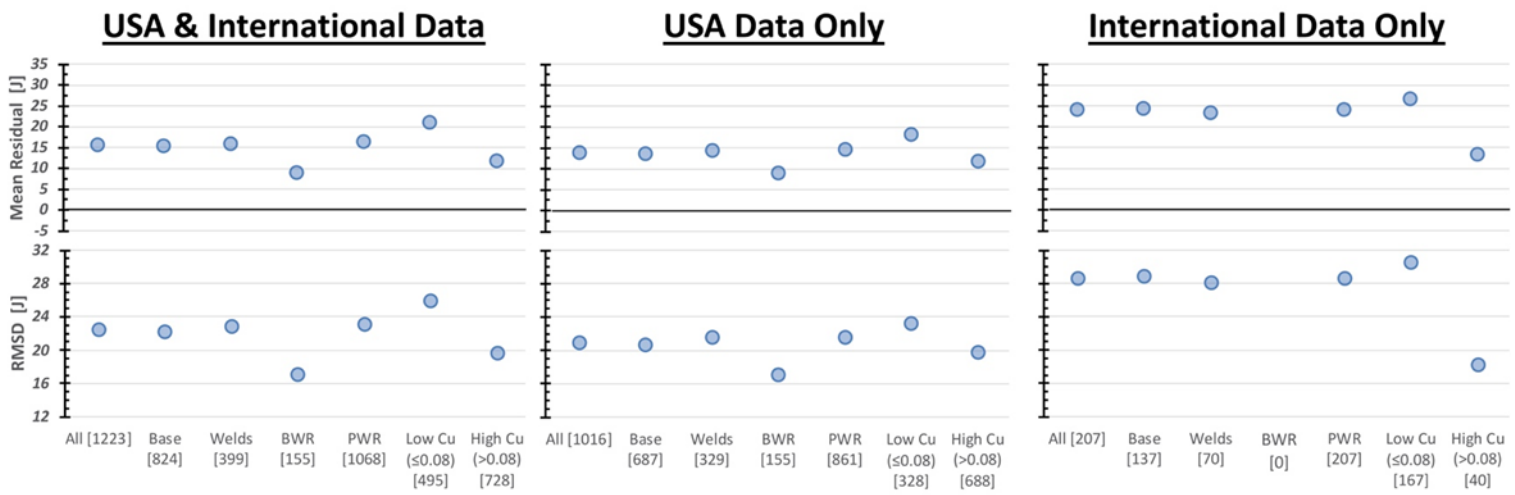

Figure 3-2. Values of mean residual (upper graphs) and root-mean square deviation (lower graphs) for the RG1.99 upper shelf energy drop predictions using different data partitions.

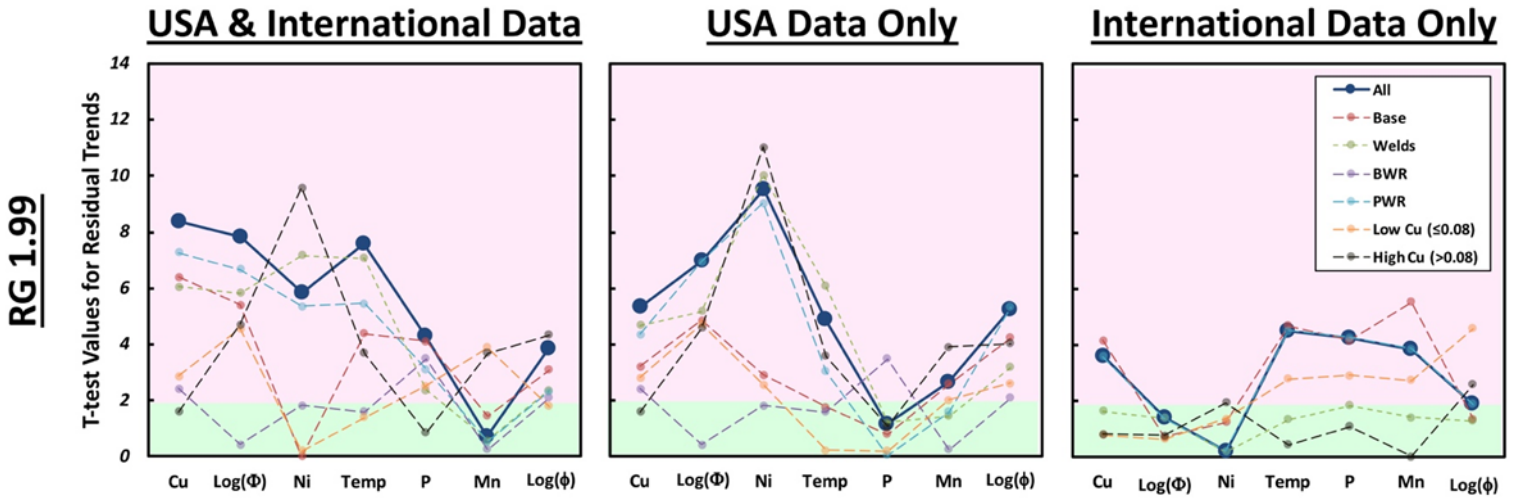

Figure 3-3. T-test values to assess residual trends relative to different regressor values and data partitions for the RG1.99 upper shelf energy drop predictions. Red shaded regions indicate statistically significant residual trends.

3.4 Fleet Impact

The fleet impact of RG1.99 ΔUSE is subtler than ΔT_{41J}. The primary impact stems from the requirements of 10 Code of Federal Regulations (CFR) Part 50 Appendix G, "Fracture Toughness Requirements" that requires plants maintain an USE energy greater than 68J[2] (50 ft-lbs) or demonstrate that a lower value of USE will provide sufficient margins of safety against fracture, consistent with American Society of Mechanical Engineers (ASME) Boiler and Pressure Vessel Code (BPVC), Section XI, Appendix G. These demonstrations are typically called "equivalent margins analysis (EMA)" and require NRC approval. The 68J (50 ft-lbs) criterion was created to be quite conservative. Consequently, reaching this criterion is not considered an indication that immediate action is required; rather it indicates that further analysis should be conducted.

In a 2010 paper [Kirk 2010] the authors compared then available data from U.S. RPV surveillance programs to the prediction of RG1.99 and produced the plot reproduced here as Figure 3-4. Figure 3-4 indicates that ≈ 19 percent of the then-available data exhibit a greater reduction in upper shelf energy than predicted by RG1.99.

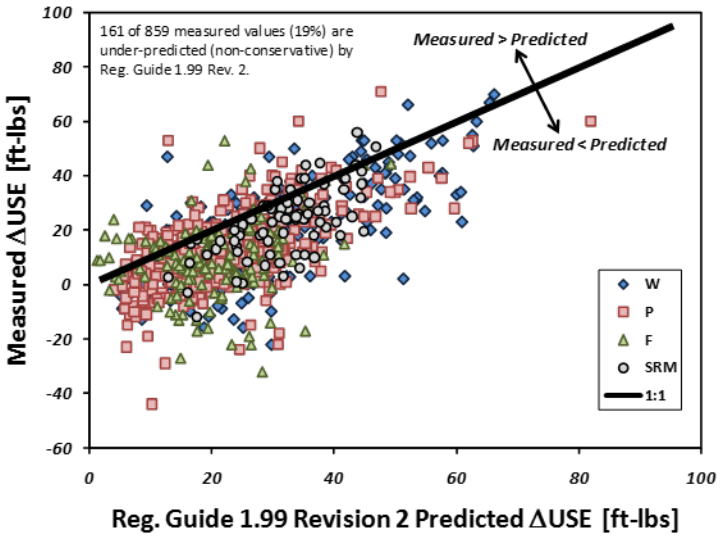

Figure 3-4. Comparison of U.S. surveillance data available in 2010 for ΔUSE with RG1.99 predictions. In the plot, W=weld, P=plate, F=forging, SRM=standard reference material.

The potential safety margin impact stems from situations where USE is predicted to exceed 68J (50 ft-lbs) but is in fact below 68J (50 ft-lbs). All other cases would either be conservative or have been deemed acceptable through approval of an equivalent margins analysis (EMA). Extended periods between surveillance material testing increase the likelihood that this condition may exist as USE predictions from RG1.99 contain significant uncertainty and residuals potentially overcoming the conservative bias of the predictions. To illustrate this, the residuals between measured and predicted $USE_{(I)}$ were plotted in Figure 3-5. Data falling to

[2] This value is defined in [ASTM E185-82] through citation of ASTM Methods A370, "Methods and Definitions for Mechanical Testing of Steel Products" and E23, "Methods for Notched Bar Impact Testing of Metallic Materials."

the right of the red line but below the blue line constitutes measured data that should have triggered an EMA but would not have been predicted to trigger an EMA; the shaded area of the plot indicates where data falling into this condition would lie. As plant fluences increase, some additional materials may transition into the lower right quadrant of Figure 3-5 depending on the specific combination of capsule withdrawals and licensing actions.

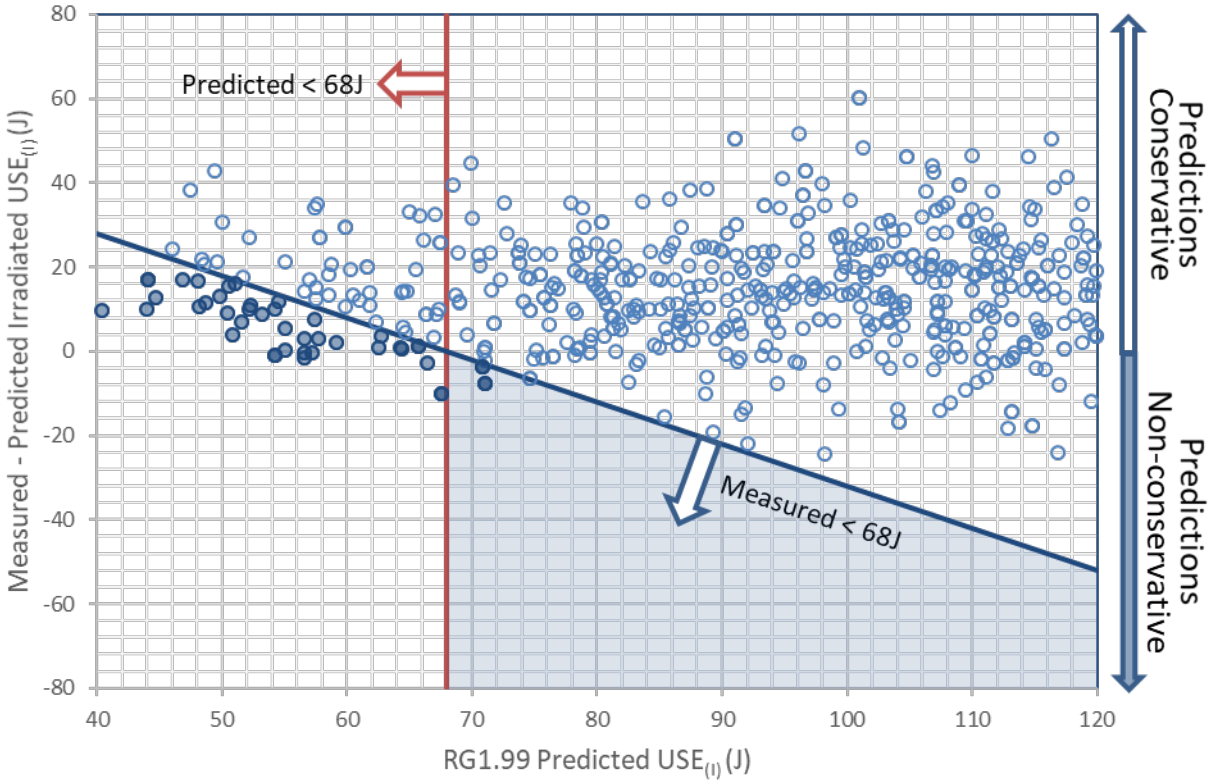

Figure 3-5. Comparison of Predicted $USE_{(I)}$ to residual of Measured – Predicted $USE_{(I)}$. Filled data represent measured $USE_{(I)}$ below 68J.

For this assessment, a preliminary estimate of the number of reactors that may fail the 68J (50 ft-lbs) criterion if measured but are not predicted to do so was conducted. Seven reactors were identified[3] (a further four reactors identified plan to cease operation imminently as of 2019). Of these, three had implemented equivalent margins analyses. The remaining four all had approved USE calculations from license renewal applications with staff verifying their calculations. These plants warrant further review.

It is unlikely for new reactors - for which high initial USE values have been specified by their designers - that the safety significant situation described above will occur until subsequent license renewals for plant operation beyond 60 years. New reactors will be aided in this by material surveillance requirements that will ensure the existence of heat-matched USE data.

[3] This was accomplished by comparing RG1.99 predictions against those from a more modern trend curve familiar to the staff [Kirk 2010]. This trend curve was selected as a representative "modern" curve; this selection was made as a convenience. The date at which the subject plants would drop below 68J (50 ft-lbs) was estimated with only two reactors having this date in the future (2025 and 2028 respectively).

Plant-specific data supports the use of RG1.99 Position 2.2 although the issues with credibility determination as discussed in Section 4 may preclude this. The effect of RG1.99 Position 2.2 is to plot a new curve on RG1.99 Figure 2 parallel to the existing curves and bounding the credible measured USE values. This is philosophically similar to the chemistry factor (CF) refit conducted under RG1.99 Position 2.1 for ΔT_{41J}. Both adjustments presume the adequacy of the curve-shapes in RG1.99 resulting in data adjustments being bias adjustments. Consequently RG1.99 Position 2.2 does not address situations where measured data contradicts the predicted curve-shapes of RG1.99 Figure. 2.

3.5 **Summary**

The RG1.99 predictions of ΔUSE contain conservative bias, significant uncertainty, and significant residuals relative to input variables. The impact on the operating fleet and new reactors that may be constructed is unclear as two acceptance paths exist (i.e., maintaining USE greater than 68J [50 ft-lbs] during licensed operation, or conducting an EMA). Further work is needed to evaluate the regulatory significance of the current 68J criteria and to determine if it should be retained, modified, or eliminated. That evaluation is outside the scope of this assessment.

4. Credibility Criteria and Use of Credible Surveillance Data

A set of credibility criteria is presented in Section B of RG1.99. These credibility criteria are presented to ensure that data used to improve the predictions of RG1.99 are appropriate for that use. If the data are deemed credible, then RG1.99 Regulatory Positions 2.1 and 2.2, defined below, may be used to adjust predictions and, in the case of Position 2.1, reduce the magnitude of margin. Five criteria are defined in Section B of RG1.99:

1. Materials in the surveillance capsules should be those judged most likely to be controlling regarding radiation embrittlement according to the recommendations of this guide.
2. Scatter in the plots of Charpy energy versus temperature for the irradiated and unirradiated conditions should be small enough to permit the determination of the 30-foot-pound temperature and the upper-shelf energy unambiguously.
3. When two or more sets of surveillance data are from one reactor, the scatter of ΔT_{41J} values about a best-fit line drawn as described in Regulatory Position 2.1 normally should be less than 15.6°C (28°F) for welds and 9.4°C (17°F) for base metal. Even if the fluence range is large (two or more orders of magnitude), the scatter should not exceed twice those values. Even if the data fail this criterion for use in shift calculations, they may be credible for determining decrease in upper-shelf energy if the upper shelf can be clearly determined, following the definition given in ASTM E 185-82.
4. The irradiation temperature of the Charpy specimens in the surveillance capsules should match vessel wall temperature at the cladding/base metal interface within ±13.9°C (25°F).
5. The surveillance data for the correlation monitor material in the surveillance capsules should fall within the scatter band of the data base for that material.

Although “scatter” is not explicitly defined in RG1.99, the Wichman presentation [Wichman 1998] determines scatter as the absolute value of the difference between the ΔT41J measurement and the RG1.99 Eq. 2-1 prediction where Eq. 2-1 has been fit, using least-squares, through the ΔT41J data.

RG1.99 Position 2.1 allows for the modification of the prediction of ΔT_{41J} as follows, if 2 or more credible surveillance data are available:

- Mean embrittlement trend: The relationship between ΔT_{41J} and fluence is fit using least squares based on "credible data." This fit defines a chemistry factor, CF_{FIT}, that is used in preference to the CF values based on the tables in RG1.99.
- Uncertainty in the future embrittlement trend: The uncertainty associated with future irradiated observations of ΔT_{41J}, the σ_{Δ} values, are halved relative to the values used when credible data is not available.
- Population of data considered: Data from "sister plants" (i.e., other operating plants having a weld fabricated from the same weld wire heat as the subject plant) are assumed to be relevant to the subject plant. While this is not in RG1.99 it is discussed in the Wichman presentation [Wichman 1998] due to being explicitly addressed in 10 CFR 50.61 (which incorporates much of RG1.99 as a regulation). These data, after adjustment for differences in chemical composition and irradiation temperature, are included in the assessment of the subject plant as if they came from the plant itself.

Position 2.2 allows for the modification of the prediction of ΔUSE as follows:

- Mean USE reduction: A curve is drawn parallel to the existing curves in RG1.99 Figure 2 "as the upper bound" of the credible surveillance data. ΔUSE is then predicted using this new curve.

4.1 Credibility Criteria

The credibility criteria are meant to allow for prediction adjustments based on plant-specific data that are within RG1.99 trend curve scatter bands. A user first determines whether their data are "credible" by applying the five criteria listed above. As written, the criteria are open to interpretation. A strict reading of the criteria may lead a user to exclude data with a single outlier as judged by refitting the chemistry factor and checking the results against the standard deviation values given in credibility criteria #2. The Wichman presentation [Wichman 1998] explicitly notes that a single outlier does not invalidate a data set. The method outlined in the presentation may not be consistent with modern statistical practice. Regardless, the result of this construction is that as more data is collected, the likelihood of one or more apparent outliers increases. The outlier(s) may render the data non-credible and the credibility criteria are therefore biased against validating larger data sets. Should the data be deemed non-credible, the user is directed to discard the chemistry factor refit losing what may be a superior data-based fit of the RG1.99 trend curve.

A further deficiency is made clear by the above: application of the credibility criteria and the use of credible data both presuppose the form of the RG1.99 trend curve and privilege this over the data. The question posed by the credibility criteria is equivalent to: "Does your plant-specific data conform well to the form of the RG1.99 trend curve?" If the answer to this question is yes, then the user must use the refit predictions if they result in higher adjusted reference temperatures and may reduce the magnitude of the margin term added to their adjusted reference temperature. If the answer to this question is no, the user must default to using the generic trend curve.

This poses a difficulty: what if the user failed the credibility criteria because the subject material embrittlement *does not conform to the shape of the RG1.99 trend curve*? In this case the user is directed back to the RG1.99 trend curve with increasing likelihood as more data is gathered

that contradicts the RG1.99 trend curve. One would also expect such material embrittlement behavior at the edges (or beyond) of the interpolation zone of the data used to generate RG1.99. This is a credible situation, for example the slope behavior of a more modern approved trend curve, 10 CFR 50.61a, does not match that of RG1.99 yet is considered to have better predictive performance overall than RG1.99 (for PWRs). Candidates for materials falling into this category include those with residuals as noted in Sections 2 and 3 of this report; and those with notably low or high operating temperatures.

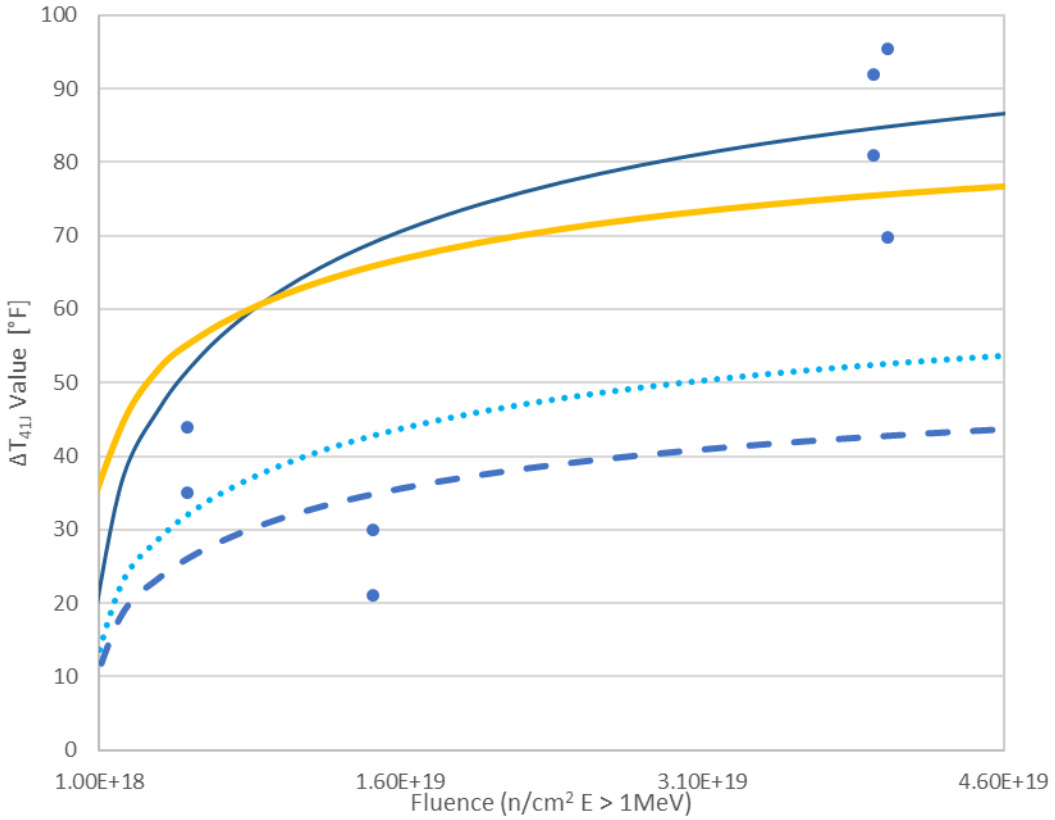

Figure 4-1. Illustration of measured plant data and application of credibility criteria. Blue dots – measured data (two sample orientations for each fluence, LT and TL). Blue curves - dotted line represents RG1.99; dashed line refit CF to the first two capsules; solid line refit CF to all measured data. Yellow curve – RG1.99 with degree-per-degree adjustment.

An example of the capabilities of the credibility criteria and adjustment process is illustrated in Figure 4-1. As is evident, even if all the data had been deemed credible (which it would not be), the refit curves would not have predicted well the embrittlement behavior of this actual plant material between the second and third sets of data. This material had an operating temperature at the bottom of the range of RG1.99 and consequently one would expect it to diverge from the shape of the RG1.99 embrittlement curve. The yellow curve illustrates a bias adjustment produced by implementing the degree-per-degree adjustment.

Several simulations were conducted to confirm the conceptual evaluation discussed above. The first set of simulations were designed to illustrate how the single outlier criteria interacts with increasing data. The second set of simulations were designed to illustrate how a plausible material (as defined by using 10 CFR 50.61a predictions) may fail the credibility criteria and the user be improperly directed back to the RG1.99 trend curve form (sans chemistry factor fit).

The following steps were conducted for the simulations first using RG1.99 and then 10 CFR 50.61a trend curves as representing the true material behavior in the simulation:

A. A defined mean trend curve (dashed curve, using RG1.99 or 10 CFR 50.61a trend curve) is selected to reflect a steel composition and product form.
B. Data sets of 2, 3, 4, or 5 ΔT_{41J} values are simulated from this defined curve by randomly sampling the scatter about the mean curve at fluences that correspond to a capsule withdrawn per the schedule defined by ASTM E185-82. Simulated plants with higher CF have more capsules in accord with ASTM E185-82.
C. CF_{FIT} is estimated from these simulated ΔT_{41J} using RG1.99 procedures (i.e., least squares fitting).

This process is illustrated in Figure 4-2.

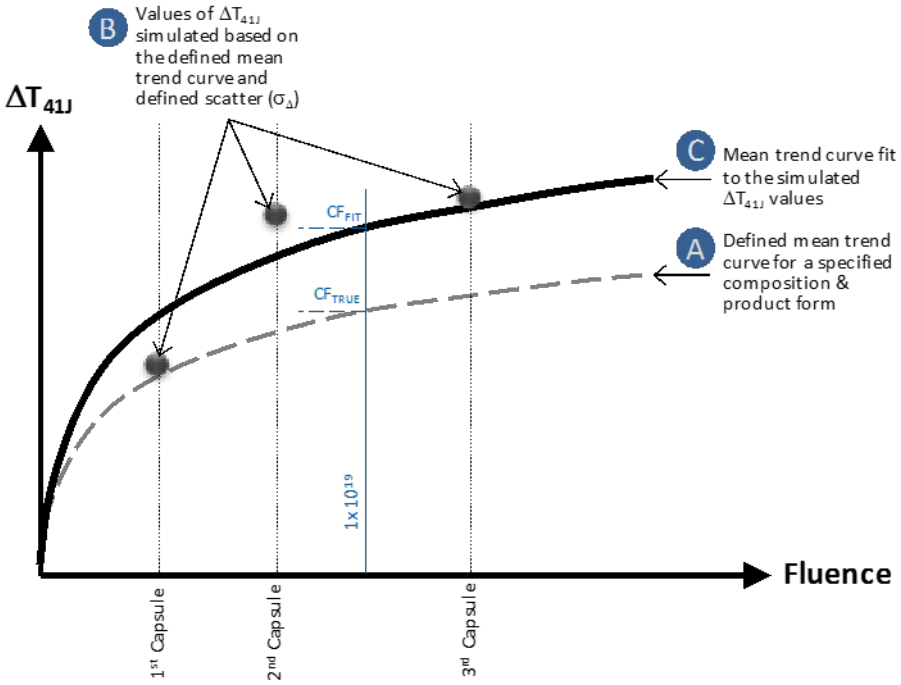

Figure 4-2. Illustration of simulation process.

Material characteristics were otherwise taken from the data used in Section 2 of this assessment. The values used are shown in Appendix A. By conducting the above through many trials, the behavior of the credibility criteria can be numerically assessed.

4.2 Use of Credible Surveillance Data

The results of these simulations are presented in Figure 4-3 through Figure 4-6. For each parameter set, 1000 simulations were conducted. The top figures of each plot, "Credible CF" indicate the percentage of simulations that were deemed credible (with a single outlier test) through the criteria at each simulated surveillance capsule test. Beneath these values, the "$CF_{SIM} < CF_{defined}$" percentage indicates how many of a given capsule had a simulated CF beneath the defined CF (due to the scatter). The defined CF is shown as $CF_{defined}$ on the vertical axes. The simulated CF_{SIM} are arranged by °C on the vertical axis while the number of

surveillance capsules tested is shown on the horizontal axis. The plot labels (e.g. “Low Cu Plate”) correspond to the properties shown in Appendix A.

For the simulations using the RG1.99 trend curve, two significant results are illustrated. First, the credibility criteria reject *more* simulated datasets as the number of data points increases. As an application of statistics, this is the opposite of a desired effect. Second, the credibility criteria discount counter-evidence more strongly as more counter-evidence is acquired. In this case, counter-evidence is constructed directly from RG1.99 as written. These results confirm a major flaw in the credibility criteria.

For the simulations using the 10 CFR 50.61a trend curve, the credibility criteria reject data more readily. This is appropriate to the credibility criteria design assumption that the RG1.99 trend curve is correct. However, it is a poor characteristic given that there are known residuals in the RG1.99 trend curve, particularly for copper, nickel, and temperature.

These results indicate that the credibility criteria promote the use of the RG1.99 trend curve over plant-specific data and do so more strongly as more plant-specific data is acquired. An increasing trend to reject plant-specific data as more becomes available implies underlying statistical issues with the credibility criteria. Applying the Wichman 1998 [Wichman 1998] approach would reduce the rejections of data but overall the same trend to reject data sets as more data becomes available would still occur.

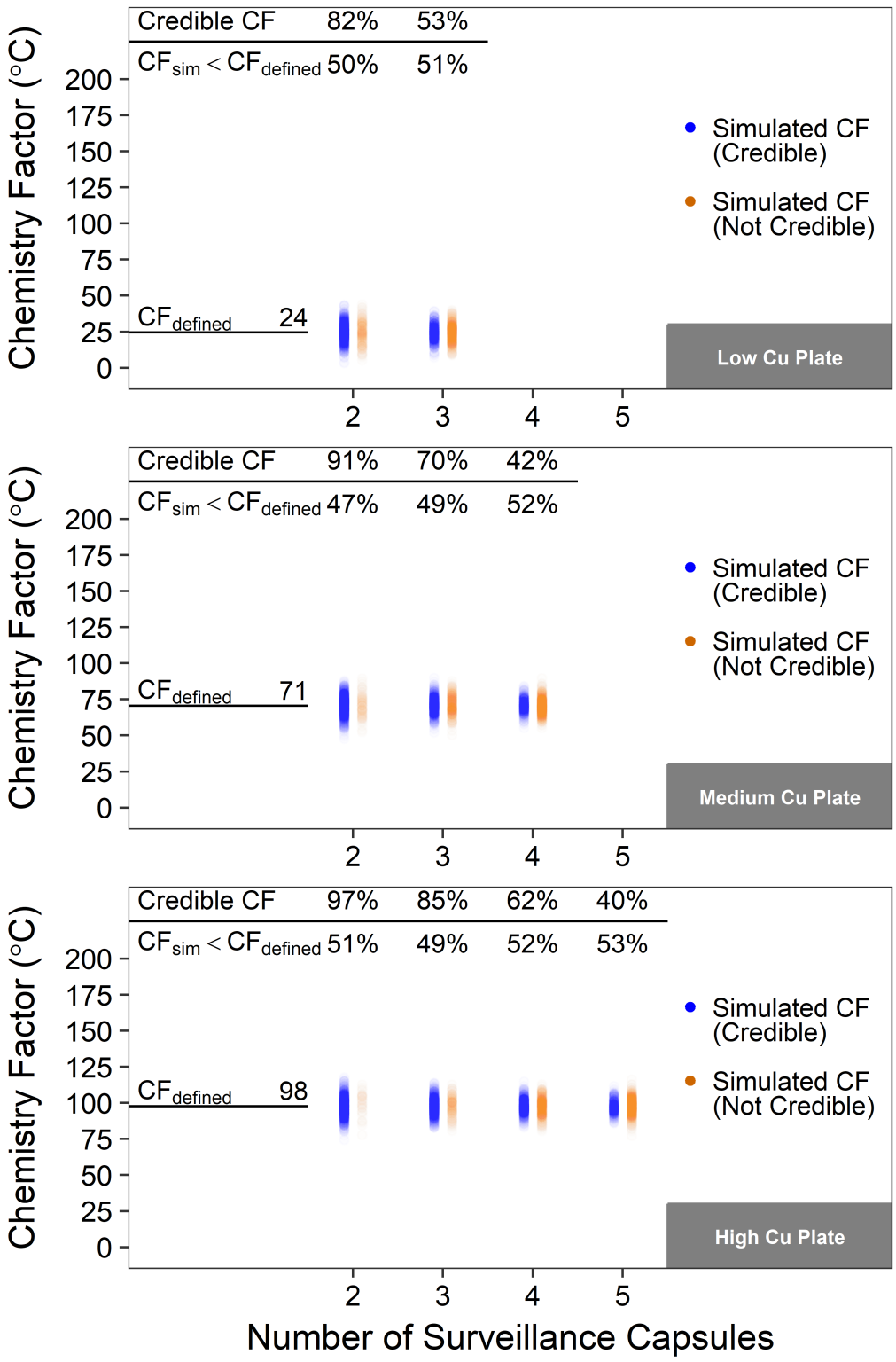

Figure 4-3. Results for Simulation Set 1 (RG1.99 provides the *defined* mean trend curve), Base Metal Cases (as defined in Appendix A)

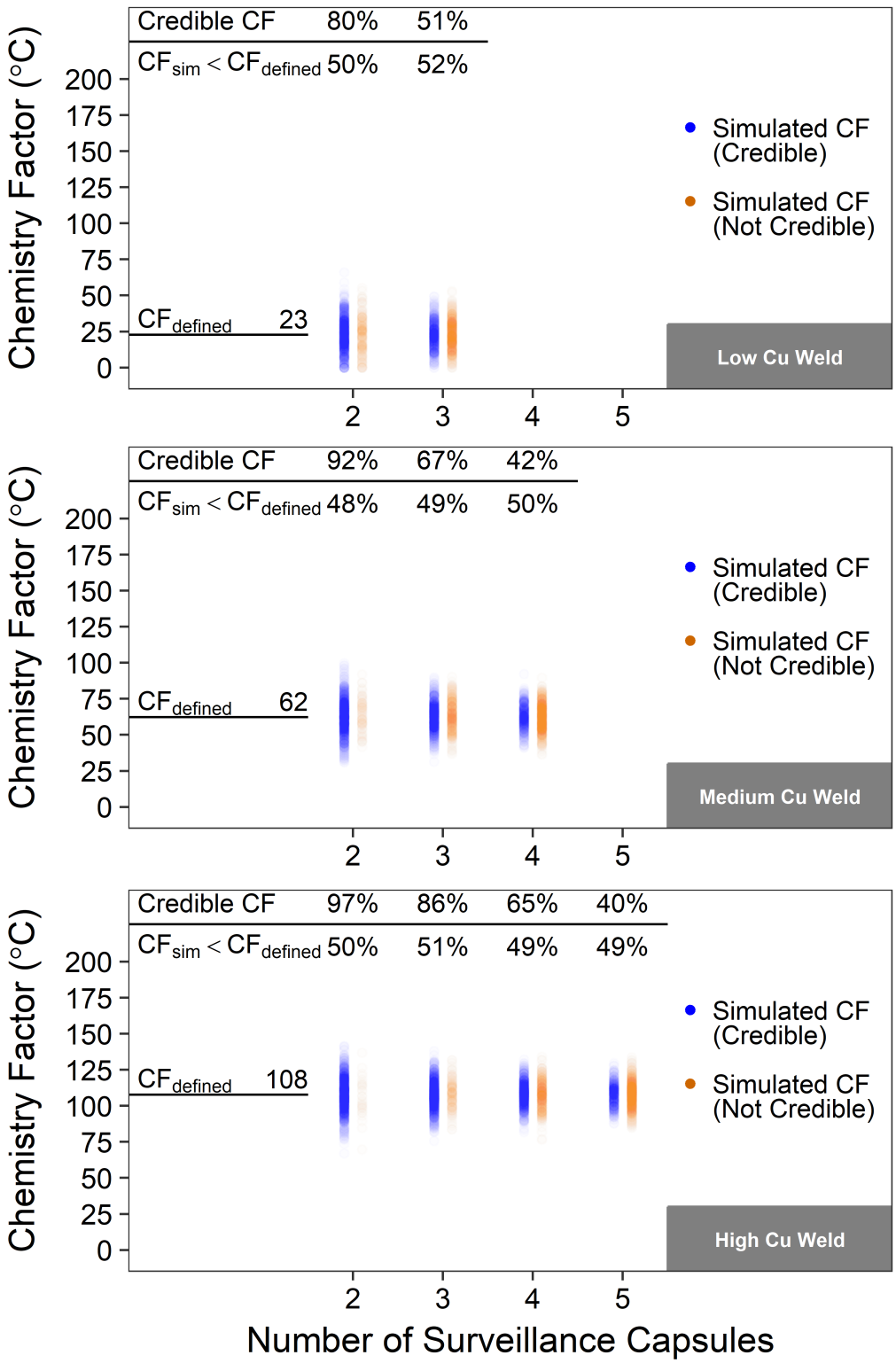

Figure 4-4. Results for Simulation Set 1 (RG1.99 provides the defined mean trend curve), Weld Metal Cases (as defined in Appendix A).

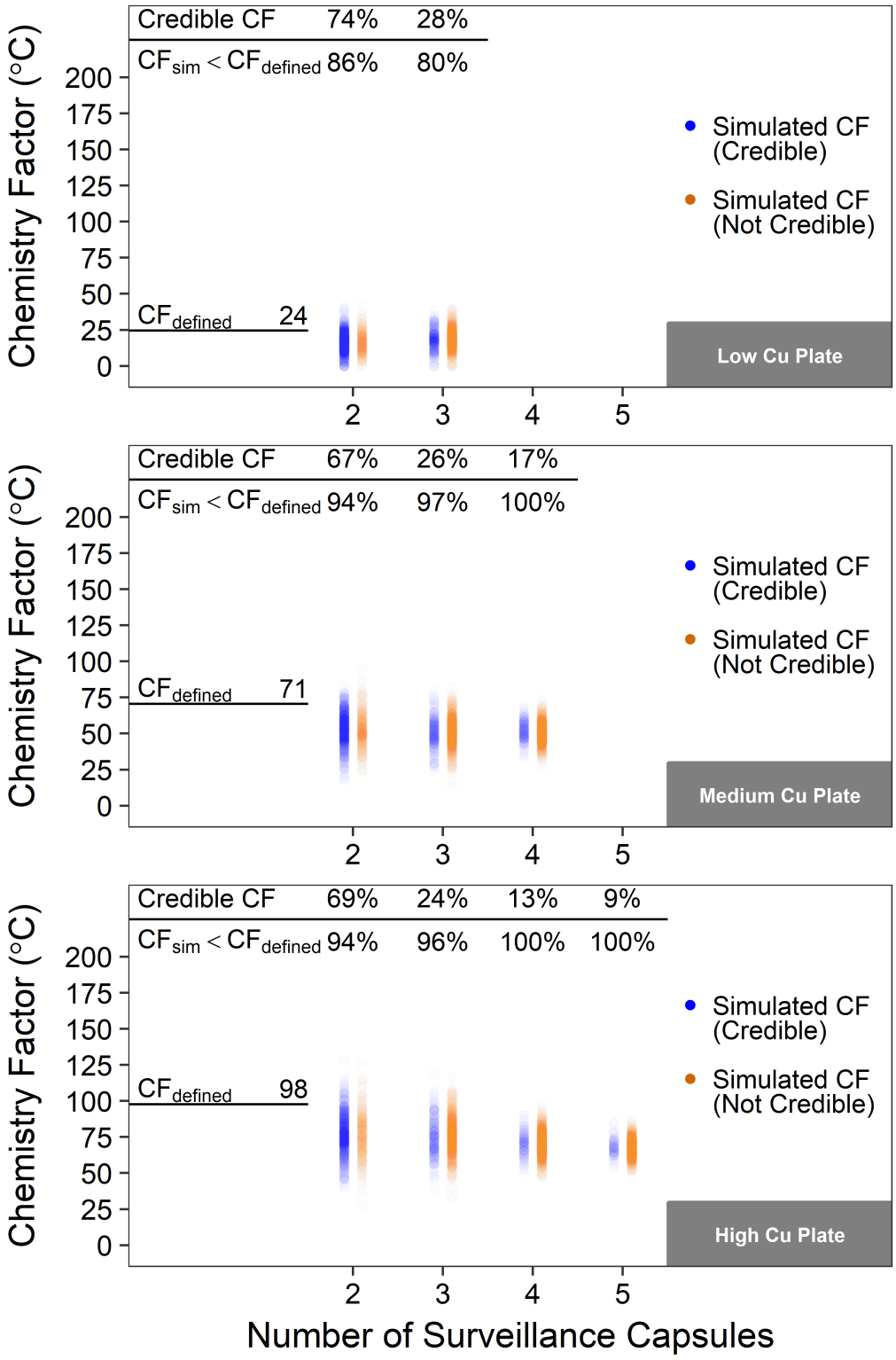

Figure 4-5. Results for Simulation Set 2 (10 CFR 50.61a in Appendix A). Base Metal Cases (as defined in Appendix A).

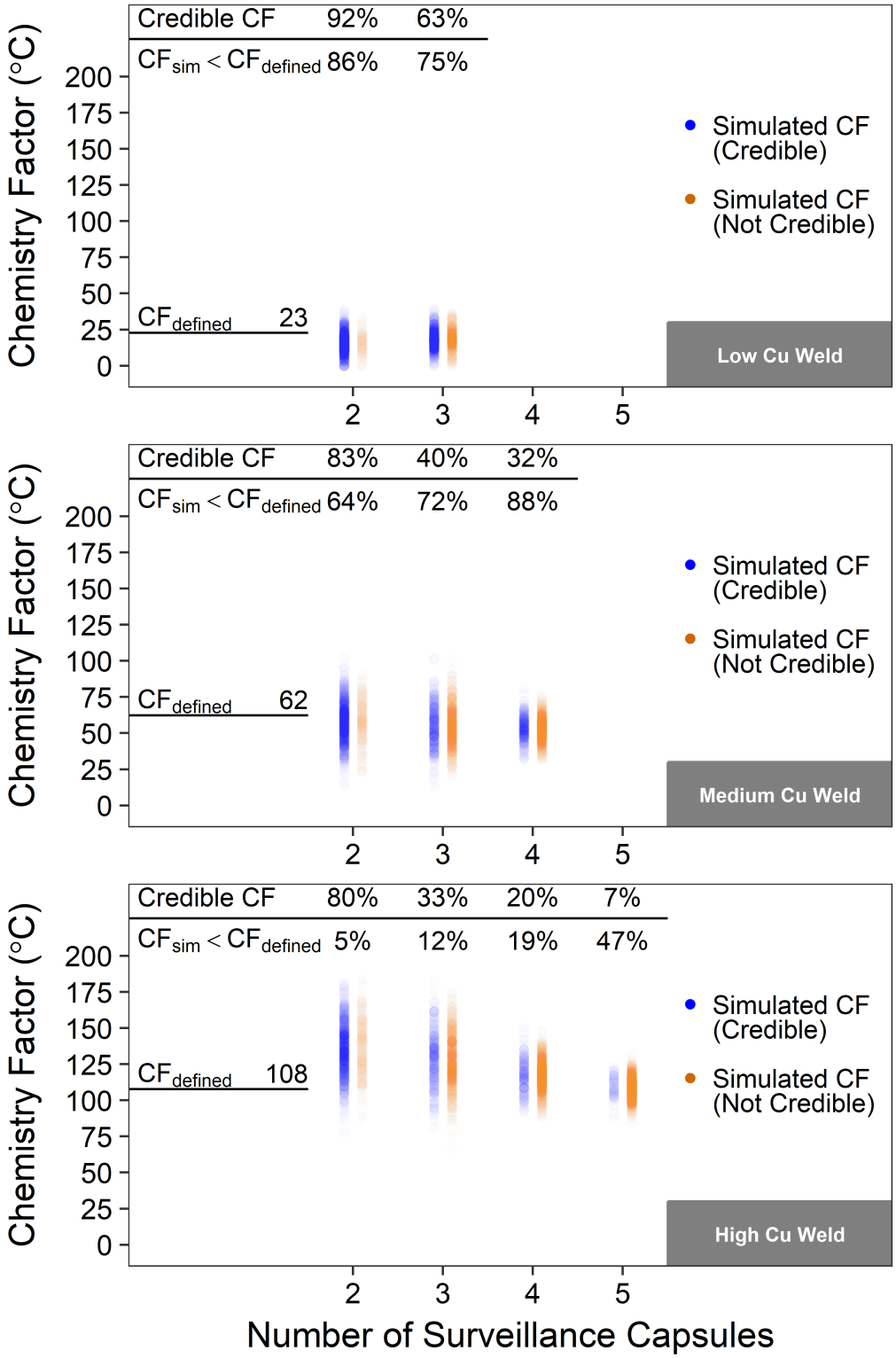

Figure 4-6. Results for Simulation Set 2 (10 CFR 50.61a provides the defined mean trend curve), Weld Metal Cases (as defined in Appendix A). High Cu results stem from 50.61a trend curve behavior for welds predicting higher embrittlement at lower fluences relative to RG1.99 (in this case converging near the final capsule fluence).

4.3 Reduction of Uncertainty (Margin) in Predicting Embrittlement

If the credibility criteria are met, then the user may reduce the σ_Δ margin term when estimating ΔT_{41J}. To assess whether this is appropriate, data sets from individual plants were accumulated and fit to the RG1.99 fluence formula to provide evidence on scatter about the mean trends. Many plants have only a few ΔT_{41J} measurements for individual materials. Because confidence bounds on estimates of variance are quite broad for small data sets, attention in this assessment is restricted to data sets having five or more ΔT_{41J} values.

The RG1.99 scatter, σ_Δ, and credibility criteria are shown below in Table 4-1.

Table 4-1. RG1.99 estimates of standard deviation (σ_Δ) for different product forms.

Product Form	RG1.99 σ_Δ value for no data, or for data that is not credible	RG1.99 σ_Δ value for credible data	Definition of Credible
Base Metals	9.4 °C	4.7 °C	Scatter < 9.4 °C
Weld Metals	15.6 °C	7.8 °C	Scatter < 15.6 °C
Note: As described in the Wichman presentation [Wichman 1998], 'scatter' is the maximum absolute difference between all of the ΔT_{41J} measurements in a data set and the RG1.99 prediction of ΔT_{41J} using the chemistry factor value CF_{FIT}.			

Data compiled by ASTM, which was discussed in Section 2.1, is used to support evaluation of RG1.99 recommendations on margin reduction and on sister plant data. The data used in this assessment are shown in Appendix B and reflect only those plant-specific data sets having five or more ΔT_{41J} measurements. The method of least squares was used to determine the value of CF_{FIT} for each dataset and the related σ_Δ value (see Figure 4-7 for an example).

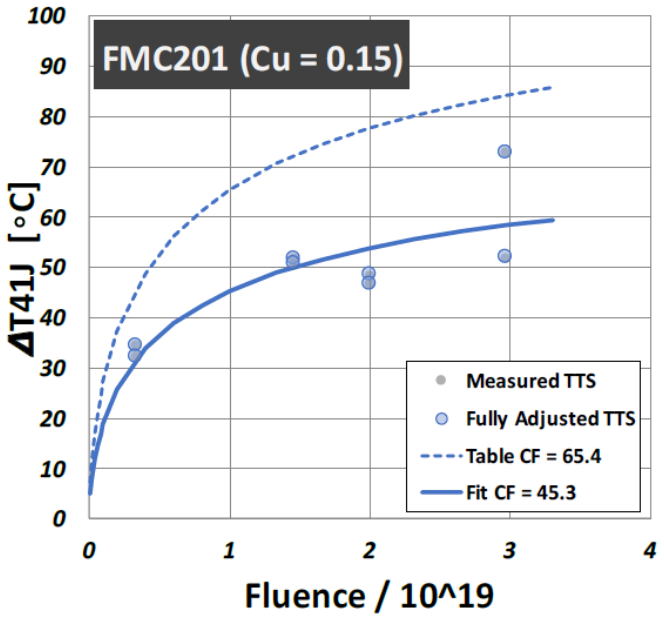

Figure 4-7. Example data set. TTS – Transition Temperature Shift.

The results are illustrated in Figure 4-8 and Figure 4-9. In the left-hand plots, σ_Δ is plotted versus the number of measurements for a given material; most measured σ_Δ estimates fall below the RG1.99 generic σ_Δ value. In the right-hand plots, σ_Δ is plotted against "scatter" as defined in RG1.99 and the note in Table 4-1. The generic σ_Δ value in RG1.99 is plotted as a thick-orange line and generally bounds the data. The σ_Δ for data that meets the credibility criteria (illustrated as the notch in the RG1.99 line) also fall below ½ the RG1.99 generic σ_Δ. In general, the σ_Δ values given by RG1.99 apply, and halving the σ_Δ used for the margin term seems reasonable. While this is true in general, it is not true universally. In addition, no record exists of the derivation of reducing the scatter for σ_Δ when credible data is available. It is possible that this is a crude application of Empirical Bayes or a direct result of standard deviation calculations for the margin term, but the basis for this reduction in margin appears to be engineering judgement.

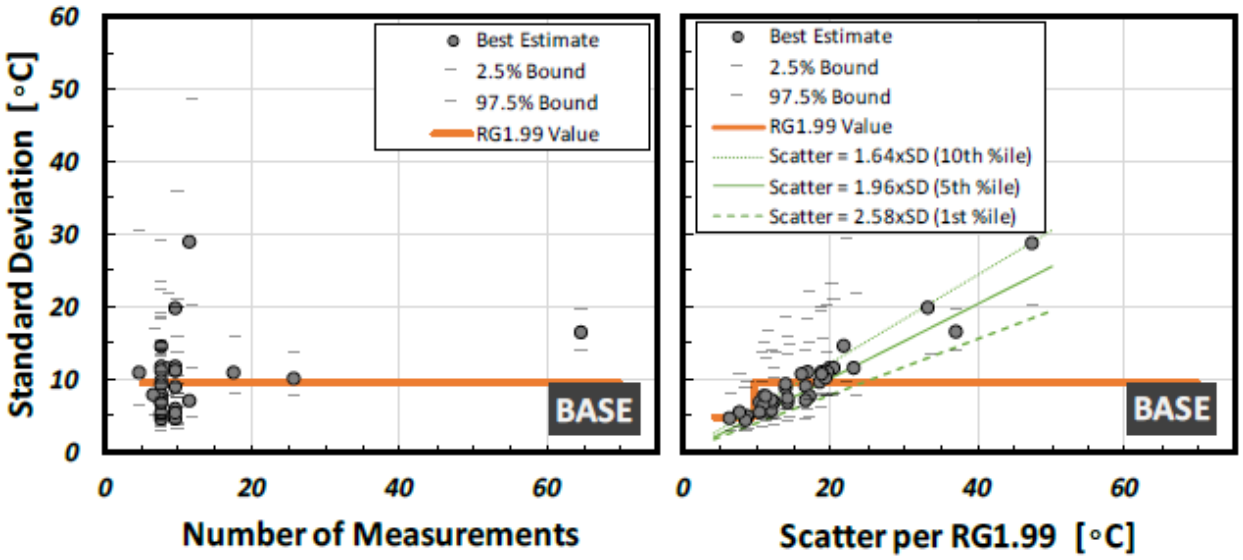

Figure 4-8. σ_Δ values for base metal.

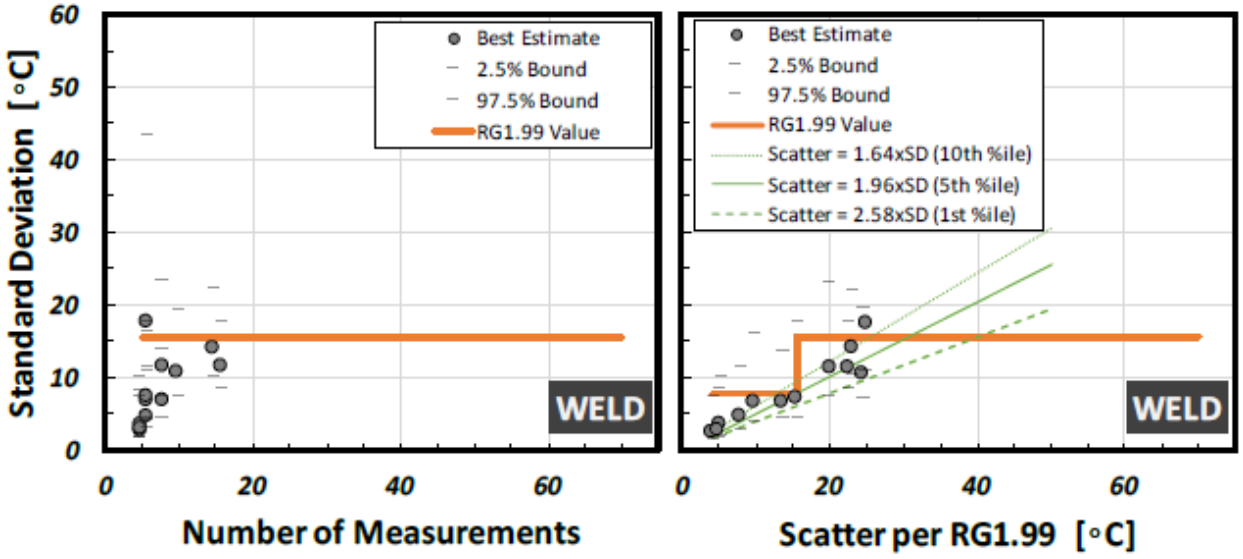

Figure 4-9. σ_Δ values for weld metal.

4.4 **Fleet Impact**

The credibility criteria are more likely to be failed when more data are obtained and/or the material does not embrittle as predicted by RG1.99. When the credibility criteria are not fulfilled, the user of RG1.99 is directed to use the RG1.99 predictions. This has potential fleet impacts in that failing the credibility criteria is quite likely *both with increased surveillance testing for data that should be highly consistent with RG1.99*, and when the material behavior *does not match the RG1.99 predictions*.

For operating reactors, it is likely that much of the negative impact of the credibility criteria has been amended by plant-specific analysis through implementation of the recommendations of the Wichman 1998 presentation [Wichman 1998]. Consequently, additional compensatory corrections for operating reactors may be unneeded. For the specific case of new reactor designs with unusual irradiation temperatures, the credibility criteria are likely to produce wholly incorrect results and consequently are of little utility. Overall new reactors will have superior initial properties, and fewer surveillance capsules. Consequently, the practical effect of the credibility criteria regarding operating windows in pressure-temperature limits and hydrostatic testing temperatures may be less burdensome, although these effects are not analyzed in this assessment. A similar consequence may result due to residuals for new reactors related to the low Cu materials employed.

4.5 **Summary**

The credibility criteria do not perform well. The criteria do not serve to indicate or manage plant specific data that credibly illustrate material behavior inconsistent with the trend curve. The performance of the credibility criteria degrades when (a) more plant-specific data are available, and (b) the plant materials are poorly predicted by RG1.99.

5. Attenuation

The RG1.99 neutron attenuation formula for fluence at a given depth through the reactor pressure vessel (RPV) wall is given in RG1.99 Equation 3. Equation 3 is reproduced here,

$$f = f_{surf}(e^{-0.24x}) \tag{5-7}$$

Where f_{surf} is the fluence at the inner surface of the RPV in 1x 10^{19} n/cm^2 (E > 1MeV), and x is the radial distance from the inner diameter of the RPV to a location of interest inside the RPV wall, in inches. Results concerning the adequacy of the attenuation formula are presented.

This attenuation formula is commonly used to enable prediction of material properties at the ¼-T and ¾-T locations in the RPV (one-quarter and three-quarters through wall thickness respectively). The formulation of the RG1.99 attenuation formula was derived from dpa-based neutron transport calculations, even though the formula inputs and outputs are in units of n/cm^2 (E > 1MeV). This assessment compares the formula to results derived from more recent dpa-based neutron transport calculations, as well as results based on mechanical property testing of actual material.

It has been noted by members of the NRC/NRR Division of Safety Systems that this formula is not applicable to regions of the reactor vessel that are not horizontally adjacent to the fuel and that are not essentially cylindrical. Therefore, for areas such as the RPV nozzles, and areas not

horizontally adjacent to the fuel, a different correlation should be applied. These limitations are not specified in RG1.99, because materials not adjacent to the active fuel were not a concern at that time. The results of this assessment are consistent with these claims as detailed below.

It should be noted that, to date, new reactor applications have conformed to operating reactor design parameters to the extent that where the attenuation formula applies to operating reactors it should apply equally well to new reactors. Such parameters include selection of materials, fluence spectra, arrangement of fuel, etc.

5.1 Assessment of RG1.99 Formula via Neutron Transport Calculations

Several evaluations of Eq. (5-7) have been made since its publication in 1986. In MRP-56 [MRP56] English, et al. compared dpa-based attenuation calculations that had been indexed to surveillance capsule dosimetry measurements to RG1.99 estimates made using Eq. (5-7) for both Brunswick 2 (a BWR) and Palisades (a PWR) [Anderson 1996, Roberts 2000, MRP56]. For Brunswick 2, the calculated attenuation showed the RG1.99 prediction was marginally more attenuated between depths of about 10-70 percent of the RPV thickness (Figure 5-1). Similarly, for Palisades, RG1.99 was marginally more attenuated from the inner RPV surface to a depth of ¾-T Figure 5-2). For both plants, the RG formula was within ±≈10% of the dpa estimates. The azimuthal angle had little effect on attenuation for either reactor.

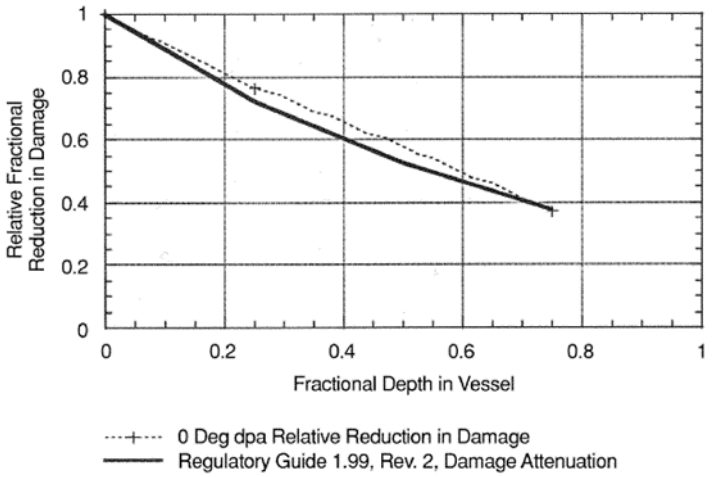

Figure 5-1. Comparison of Attenuation of Damage through Brunswick 2 BWR Pressure Vessel with the RG1.99 Prediction of Damage Attenuation [MRP56, Anderson 1996]

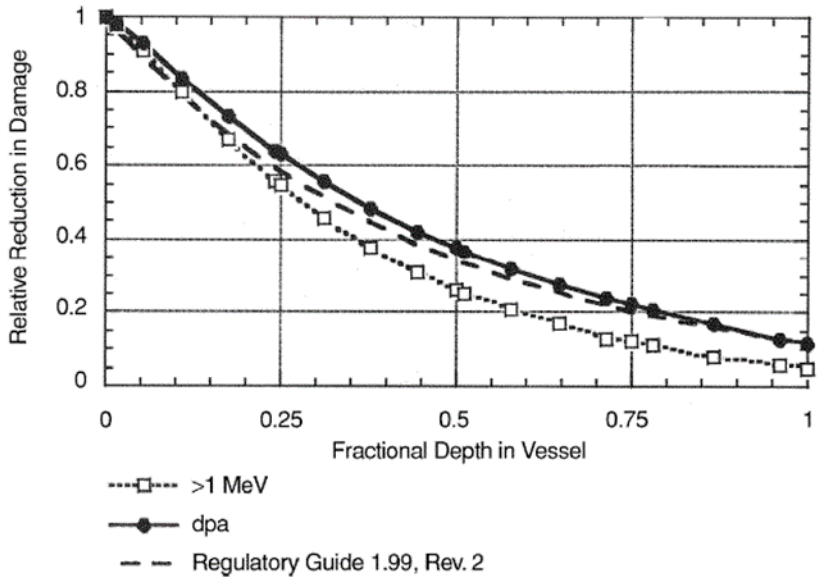

Figure 5-2. Comparison of Attenuation of Damage through Palisades PWR Pressure Vessel with the RG1.99 Prediction of Damage Attenuation [MRP56, Roberts 2000]

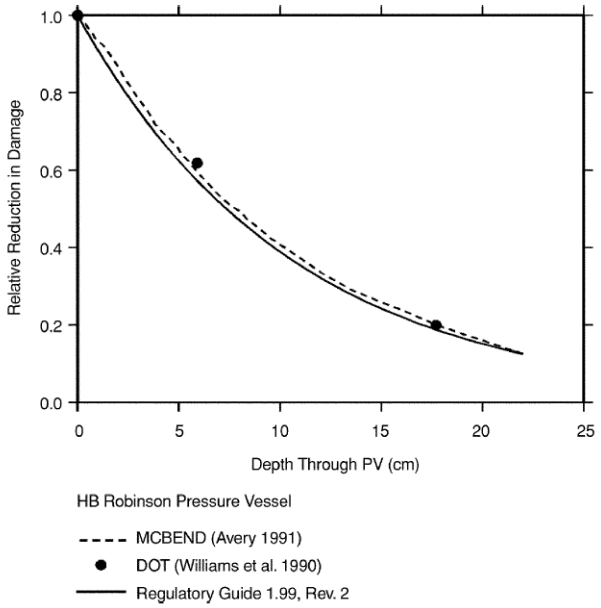

Figure 5-3. Comparison of Attenuation of Damage through H.B. Robinson PWR Pressure Vessel with the RG1.99 Prediction of Damage Attenuation [EPRI MRP56]

Avery and Williams et al. compared Eq. (5-7) to attenuation calculations for the H. B. Robinson reactor using several neutron transport codes reproduced here in Figure 5-3 [MRP56]. Results showed Eq. (5-7) differed only slightly from dpa-based predictions.

More recently, Jones compared Eq. (5-7) and the calculated dpa using the RAMA fluence methodology for three different BWR designs and two PWR designs [Jones 2012, BWRVIP 126]. Jones' comparisons were made both within the cylindrical shell course adjacent to the active fuel as well as above and below this region. Areas in the reactor shell above and below active fuel were of interest because nozzles in PWRs tend to lie above the active fuel whereas nozzles in BWRs tend to lie below. Especially during a period of extended operation, both

regions can have inner diameter fluences above 10^{17} n/cm^2 (E > 1MeV), thereby meriting evaluation [NRC 14]. Jones' calculations produced the following results:

- Adjacent to active fuel: Eq. (5-7) agreed well with the calculated dpa for all the designs, except the smallest modeled BWR, which had 368 fuel assemblies. For this small BWR the prediction of Eq. (5-7) and dpa calculations began to diverge at 40 percent of the RPV wall thickness (see Figure 5-4). Even so the maximum error of Eq. (5-7) is ≈11 percent at ¾T, and that error is conservative.
- Outside of active fuel region: In the nozzle courses, Jones observed significant and non-conservative deviations between the calculated dpa and the Eq. (5-7). At the most extreme, Eq. (5-7) under predicted the fluence by nearly a factor of seven on the outside surface of a 193 fuel assembly PWR above the core shell region (Figure 5-5)[4]. Jones concluded RG1.99 did not account for neutron cavity streaming effects, leading to the under prediction of fluence at and above the nozzle course. Attenuation in the nozzle course region is beyond the scope of this report and is the subject of an ongoing NRC research project. Preliminary results from this project, which were presented at a public meeting in 2017, agree with Jones' assessment [NRC 17].

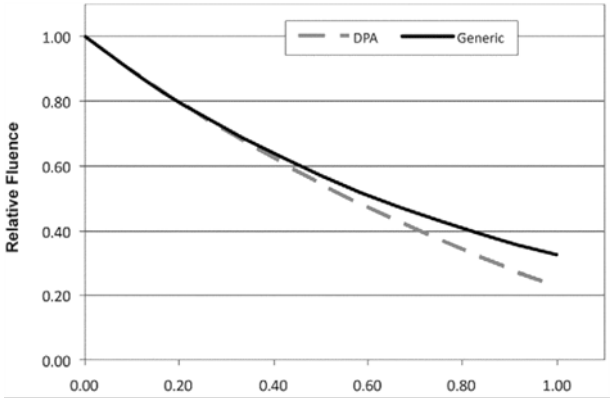

Figure 5-4. Relative Fluence Calculated Using RG1.99 (Generic) and the RAMA Fluence Methodology (dpa) Function of RPV through Wall Thickness in a 368 fuel assembly BWR. [Jones 2012]

[4] Jones' results clearly demonstrate that Eq. (5-7) is only accurate within the shell course regions adjacent to the active fuel while in the geometrically complex nozzle region is non-conservative. Nevertheless, the inner wall fluence at the nozzle course is typically low (≈10^{17} or lower) to begin with. Thus, the effect of an ~7x under-prediction of fluence on ΔT41J estimates is low (e.g., for a Cu=0.15 Ni=0.75 weld RG1.99 estimates a value of ΔT41J values of 10.2 and 32.6°C at 1x10^{17} and 7×10^{17}, respectively).

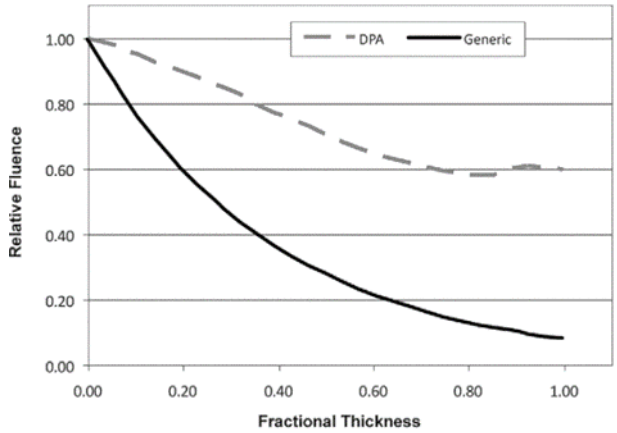

Figure 5-5. Relative Fluence Calculated Using RG1.99 (Generic) and the RAMA Fluence Methodology (dpa) as a Function of RPV through Wall Thickness in a 193 fuel assembly above the reactor core [Jones 2012].

5.2 Assessment of RG1.99 Formula via Results of Mechanical Property Testing

The second approach for estimating neutron attenuation through the RPV wall is by performing mechanical property tests (e.g., hardness, tensile, Charpy, or T_0) using samples removed from through-wall positions of either actual or simulated RPV walls. Testing is performed on decommissioned RPVs or on steel coupons arranged in series parallel to the neutron source, these being intended to simulate a RPV wall. Two examples of this type of work are as follows:

- In the 1980s, Oak Ridge National Laboratories performed attenuation studies at the Pool Side Facility (PSF) [McElroy 1986]. In the comparison to the PSF experiments, RG1.99 predicted somewhat less attenuation (a more conservative result) from the inner wall of the simulated RPV through ½-T thickness (see Figure 5-6).
- More recently, Server et al. reported on a study using 18 aligned 10 mm thick plates to simulate an RPV wall (see Figure 5-7) [Server 2010]. The plates were exposed to neutron irradiation at a temperature of 286 ± 6°C (552 ± 11°F) at a flux of $7x10^{12}$ n/cm²/s at the inside surface of the NIIAR Dimitrovgrad Russia, reactor RBT-6. A comparison of the measured neutron attenuation and corresponding ΔT_{41J} values with the RG 1.99 prediction is shown in Figure 5-8. Although some scatter clearly exists in the data, it is not inconsistent with predictions made by the coupled use of the RG1.99 attenuation formula (Eq. (5-7) and the RG1.99 trend curve.

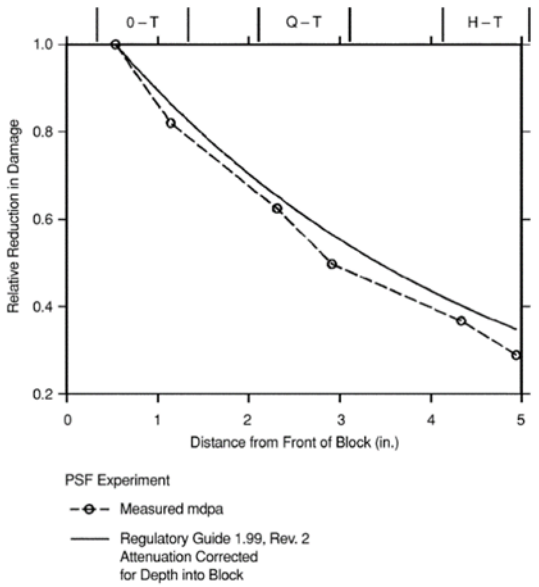

Figure 5-6. Comparison between Damage Attenuation in the Poolside Facility Experiment in the RG1.99 Attenuation Rule Corrected for the Depth of the First Specimen Layer [McElroy 1986]

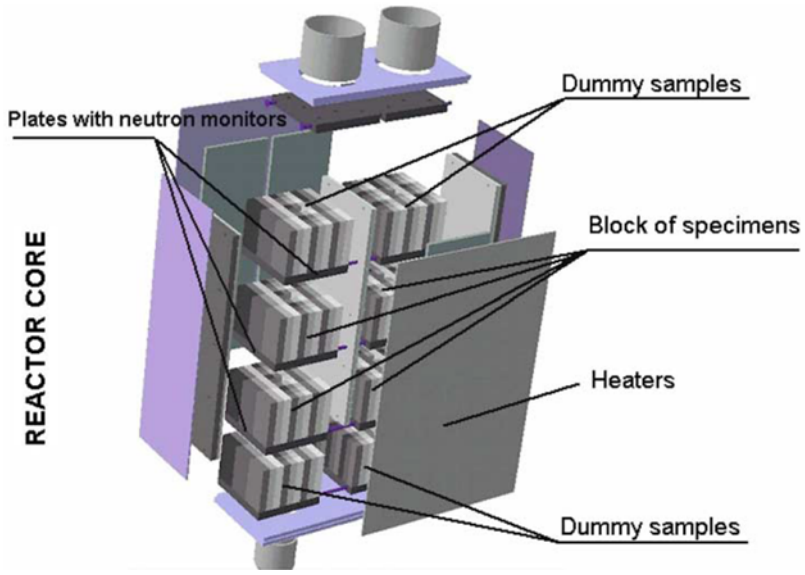

Figure 5-7. Diagram of the Simulated RPV through Wall Embrittlement Experiment [Brumovsky 06]

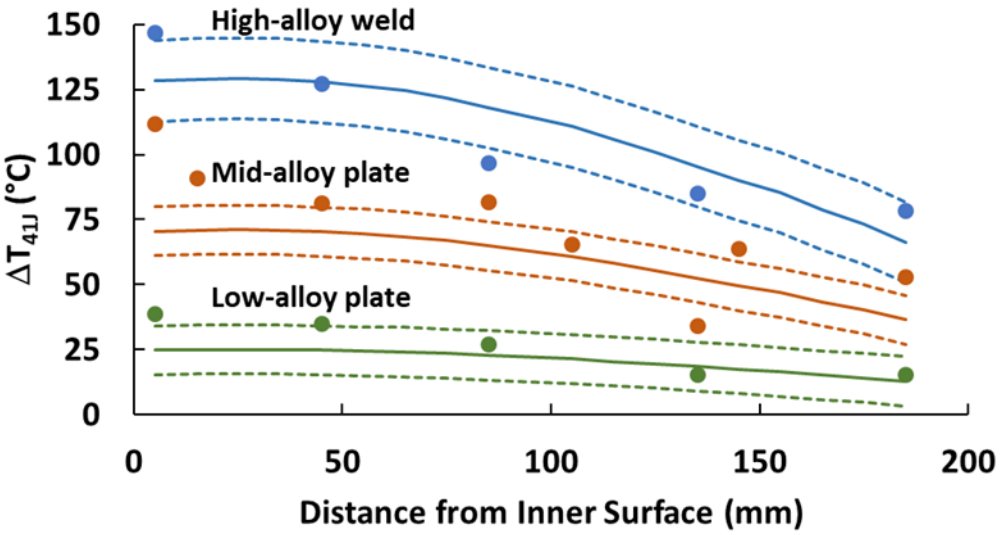

Figure 5-8. Comparison of the RG1.99 Predicted Attenuation with the Simulated RPV through Wall Experiment by [Server 2010]. Solid curves are the RG1.99 prediction based on the ID fluence as attenuated by Eq. (5-7) and then used in the RG1.99 trend curve. Dashed curves are the ±1σ uncertainty bounds (using RG1.99 values). The alloy compositions are [High weld Cu=0.30, Ni=0.58] [Mid Plate Cu=0.14 Ni=0.84] [Low Plate Cu=0.06 Ni=0.59]

5.3 Summary

The attenuation formula presented in RG1.99 continues to produce reasonable results as compared to both dpa-based modelling and experimental results for plates, forgings, and welds of a cylindrical character horizontally adjacent to the fuel region. Although the fidelity of this formula decreases markedly for areas of RPV not adjacent to the fuel core, these areas have been historically of low concern as they receive lower fluence. For the operating fleet, this is being handled in part through an effort that is addressing nozzle structural integrity research effort pertaining to fluence calculations for nozzles. The lack of limitations on the use of the attenuation formula is a deficiency. For new reactors, care should be taken if areas of interest beyond those directly adjacent to the core are limiting in some aspect, such as for Pressure-Temperature limits. The basis for applying the attenuation formula to new reactors may also require additional verification or validation if the proposed geometries, fuel patterns, and internal spacings differ significantly from those of the operating fleet. New reactor applications have not presented such difficulties to date as fuel, internals, and vessel design have been largely similar to the operating fleet.

6. Common Additions to RG1.99

Several additional practices beyond the explicit text of RG1.99 have been commonly applied. The effect of the degree-per-degree correction for temperature is discussed in Section 2. The effect of sister plant data, as motivated by 10 CFR 50.61, “Fracture toughness requirements for protection against pressurized thermal shock events,” and described by Wichman [Wichman 1998] is detailed below. In addition, the increasing fluence exposure of the fleet has brought additional elements of RPVs into consideration, specifically nozzles and materials above and below the reactor fuel, that are currently unaddressed or poorly addressed in RG1.99 (respectively).

6.1 Sister Plant Data

The Wichman presentation includes discussion of "sister-plant" data and the degree-per-degree adjustment. The degree-per-degree adjustment is discussed in more detail in previous sections. Sister plant data is used, after temperature and chemistry adjustment, as if it is plant-specific data [Wichman 1998] and is consequently subject to the credibility criteria of RG1.99. This practice is mandated in 10 CFR 50.61, which incorporates the necessary elements of RG1.99,

> *"To verify that [the T_{41J}] for each vessel beltline material is a bounding value for the specific reactor vessel, licensees shall consider plant-specific information that could affect the level of embrittlement. This information includes but is not limited to the reactor vessel operating temperature and any related surveillance program results. Surveillance program results means any data that demonstrated the embrittlement trends for the limiting beltline material,* ***including but not limited to data from test reactors or from surveillance programs at other plants [emphasis added]*** *with or without surveillance program integrated per 10 CFR Part 50 Appendix H."*

As discussed in Section 4, the credibility criteria of RG1.99 tend to reject data when more data are available. Consequently, the addition of sister plant data increases the likelihood that plant-specific data will be rejected. To assess what happens if the credibility criteria are still satisfied, sister plant data were analyzed to determine the effect of its inclusion on $\sigma_{\Delta,}$ and, consequently, whether its inclusion was consistent with the σ_{Δ} basis of RG1.99 and the reduction in σ_{Δ} granted for the use of credible data. Several candidate materials were identified (i.e. those with the same weld wire heat exposed to irradiation in more than one operating reactor). The data used are those in the red shaded cells of Appendix B. The assessment was conducted in the same manner as that conducted in Section 4 including the source of the data. The data was adjusted to the average irradiation temperature of the dataset via degree-per-degree.

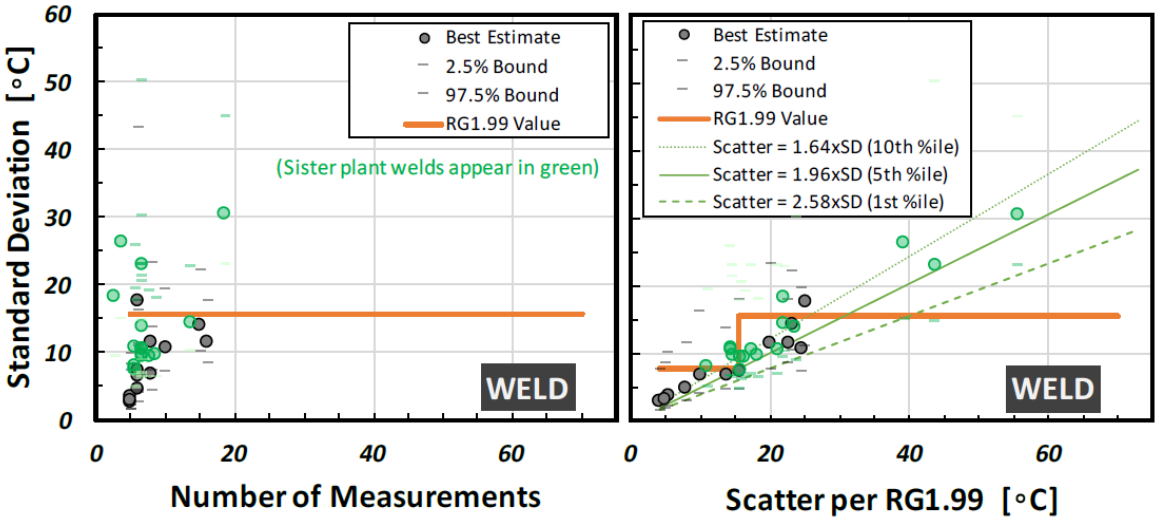

Figure 6-1. σ_{Δ} values for weld metals irradiated in individual plants (black circles, same data as in Figure 4-9) compared with sister plant weld metal data (green circles).

Figure 6-1 plots those data subsets from Figure 4-9 having sister plant data using black circles. The addition of the sister plant data and reanalysis to determine the standard deviation of the fit for each expanded dataset is indicated by the green circles. As shown in Figure 6-1, the

inclusion of sister plant data tends to increase the σ_Δ of the resultant data set. The results are as follows,

- ≈27 percent of sister plant data have σ_Δ values above the RG1.99 value for welds of 15.6°C (28°F). The σ_Δ value for these data will always be non-conservatively estimated (i.e., under-estimated) by RG1.99.
- ≈12 percent of sister plant data have σ_Δ values below the RG1.99 estimate of 7.8°C (14°F) for welds evaluated by credible surveillance data. The σ_Δ value for these data will always be conservatively estimated (i.e., over-estimated) by RG1.99.
- The remainder of sister plant data (≈61 percent) have σ_Δ values between the RG1.99 estimates for welds of 7.8 and 15.6°C (14 and 28°F).

On average, the σ_Δ of sister plant data is ~6°C (11°F) higher than for plant-specific data. Consequently, the inclusion of sister plant data will increase the likelihood that a data-set will be deemed non-credible.

The advent of small module reactor designs having multiple units of highly consistent design and manufacture at a single site presents a unique incentive to leverage sister plant data for surveillance. The lack of clear guidance in RG1.99 presents a barrier to implementation of sister plant data for this scenario. Combined with the above, this suggests that the guidance provided in RG1.99 is deficient both for operating plants and for new reactor applications.

This assessment did not seek to identify why sister plant data increases scatter. The sister plant data were adjusted to match the plant of interest through RG1.99 processes, that, as discussed above, are known to retain residuals and biases.

6.2 Materials Above and Below Fuel

RG1.99 provides no guidance regarding pertinent RPV materials including RPV nozzles and circumferential areas above and below the active fuel. The predominant factor in addressing these areas is the lack of guidance regarding the estimation of fluence, which does not follow the RG1.99 attenuation formula. This is discussed in more detail in Section 5 and is noted here for completeness. This deficiency is of concern primarily for high-fluence PWRs in the operating fleet.

7. Conclusions and Recommendations

While the performance of RG1.99 is currently adequate, all aspects of the RG merit further attention as fluence values increase, new material chemistries are used in new vessels, and new operating temperature regimes are proposed. The current revision of RG1.99 falls short of its intended function, that for which it is titled, “Radiation Embrittlement of Reactor Vessel Materials.” The benefits of having a reliable and single approach to reactor embrittlement analysis are increasingly being lost. Consequently, the efficiency and effectiveness of NRC oversight through leverage of RG1.99 will be reduced. Potential non-conservative results for high-fluence materials provide a strong indication that action is warranted in a timely fashion. It is recommended that a program to revise RG1.99 be initiated addressing the trend curves, statistical treatments, and use of plant-specific data.

The results of this assessment are summarized below. The summary distinguishes between the effects on operating fleet and new reactor applications.

7.1 **Operating Fleet**

The performance of RG1.99 has proven adequate within the interpolation of the original dataset. Previously known weaknesses of RG1.99 include performance outside of this range, specifically for high fluence, high Ni, and low Cu. This assessment confirmed these weaknesses and identified further issues. These weaknesses are compounded by the poor performance of the credibility criteria and recommended use of credible data. In addition, the utility of "sister plant" data and the degree-per-degree adjustment proved to be complicated (i.e. utility that is further degraded by the credibility criteria and related adjustments defaulting to the RG1.99 trend curve even when high-quality data may indicate this is inappropriate.

The primary deficiencies issues related to the operating fleet warranting further attention are:

- Higher standard deviation values from current data.
- Non-conservative predictions at high fluence.
- Ineffective credibility criteria.
- Needed credible data use recommendations.

The overall performance of the trend curves for ΔT_{41J} and ΔUSE could be improved, which would influence the above as well. It is predicted that these deficiencies will become a concern in the mid-2020s. This concern stems from an increasing number of plants with potentially non-conservative predictions of embrittlement for their materials due to high fluences.

The lack of authoritative guidance for topics such as the degree-per-degree and use of sister-plant data may also warrant attention beyond being an omission within RG1.99.

7.2 **New Reactors**

The performance of RG1.99 is more troublesome for new reactors primarily due to the improved initial chemistries. All new reactor designs utilize modern reactor chemistries having low Cu. The predictive accuracy of RG1.99 has proven to contain significant residuals for these chemistries. Worse, designs such as NuScale operate at temperatures outside of the limitations of RG1.99. Given that small modular reactors (SMR) designs such as NuScale include multiple (12) reactors per site, this may rapidly become a major unhandled case should multiple sites come online. The poor performance of the credibility criteria and related adjustments will be of greater consequence to new reactors. This is because they compound the issues with the RG1.99 trend curves by redoubling the reliance on curves known to be poorly fit to new reactor chemistries and conditions.

The primary areas for improvement of RG1.99 for new reactors are:

- Trend curves
- Standard deviation values
- Predictions at high fluence
- Credibility criteria
- Credible data use recommendations

While it is expected that RG1.99 results will generally be conservative relative to new reactor chemistries, this cannot be universally assumed. This is especially true for low temperature operation outside of the limitations of RG1.99.

Finally, RG1.99 currently provides no guidance relative to the application of sister plant data, or the specific application of sister-plant within integrated surveillance programs (which is more likely of interest to new reactors), a deficiency of omission. This is of interest due to SMRs that may submit ISPs and will require guidance for use of sister plant data.

Acknowledgements

The authors would like to acknowledge several individuals for their critical support. First, Dr. Mark Kirk, formerly of the NRC, produced the predominant share of the technical work reported here. Second, Dr. David Rudland, Dr. Robert Tregoning, and Mr. Jeffrey Poehler of the NRC provided substantial technical and editorial support. The authors would also like to thank their colleagues in the Offices of Nuclear Reactor Regulation and New Reactors who spent considerable time and effort reviewing drafts of this report.

8. References

ADJE090015-EA — Adjunct for E900-15 Technical Basis for the Equation Used to Predict Radiation-Induced Transition Temperature Shift in Reactor Vessel Materials, ASTM International, West Conshohocken, Pennsylvania, U.S..

Anderson 1996 — S. L. Anderson, “Analysis of 300 Degree Capsule from the Carolina Power and Light Company Brunswick,” WCAP-14774 (November 1996).

ASTM E185-82 — *Standard Practice for Design of Surveillance Programs for Light-Water Moderated Nuclear Power Reactor Vessels*, ASTM International, West Conshohocken, Pennsylvania, U.S. (revised 1982)

BWRVIP-86 1A — BWRVIP-86 Rev. 1-A: BWR Vessel and Internals Project, Updated BWR Integrated Surveillance Program (ISP) Implementation Plan, EPRI, Palo Alto, CA: 2012. 1025144.

BWRVIP 126 — RAMA Fluence Methodology Software, Version 1.2. (2010). BWR VIP-126, Revision 2: BWR Vessel and Internals Project. EPRI, Palo Alto, CA.

Debarbaris 2005 — Derbarberis, L., Acosta, B., Zeman, A., Sevini, F., Ballesteros, A., Kryukov, A., Gillemot, F., Brumovsky, M., “Effect of irradiation temperature in PWR RPV materials and its inclusion in semi-mechanistic model,” Scripta Materialia, Vol. 53, Issue 6, September 2005, pp. 769-773.

Jones 2012 — Jones, E. N., "Comparison of Regulatory Guide 1.99 Fluence Attenuation Methods," Journal of ASTM International, Vol. 9, No. 4, 2012, pp. 1-7.

Kirk 2010 — Kirk, M., “A New Relationship for Upper Shelf Energy Drop,” IAEA Technical Meeting on Irradiation Embrittlement and Life Management of Reactor Pressure Vessels in Nuclear Power Plants, Znojmo, Czech Republic, October 18-22 2010.

McElroy 1986 — W. N. McElroy (ed.), “LWR Pressure Vessel Surveillance Dosimetry Improvement Program: PSF Experiments Summary and Blind Test Results,” NUREG/CR-3320, Vol. 1 (HEDL-TME86-8), July 1986.

MD6.6 — NRC Management Directive 6.6, Regulatory Guides, May 2, 2016, available at https://www.nrc.gov/docs/ML1608/ML16083A122.pdf.

MRP56 — Materials Reliability Program (MRP): Attenuation in U.S. RPV Steels (MRP-56), EPRI, Palo Alto, CA: 2002. 1006584.

MRP326 — Materials Reliability Program: Coordinated PWR Reactor Vessel Surveillance Program (CRVSP) Guidelines (MRP-326), EPRI, Palo Alto, CA: 2011. 1022871.

NRC 87 — NRC Regulatory Analysis, Revision 2 to Regulatory Guide 1.99 Radiation Embrittlement of Reactor Vessel Materials, November 20, 1987, ADAMS ML102310298.

NRC 14 — NRC Regulatory Issue Summary 2014-11, “Information on Licensing Applications for Fracture Toughness, Requirements for Ferritic Reactor Coolant Pressure Boundary Components,” October 14 2014, ADAMS ML14149A165.

NRC 17	"Summary of U.S. Nuclear Regulatory Commission Computation of Neutron Fluence Information Exchange Public Meeting," ADAMS ML17038A134, ML17038A135 and ML17038A136.
REAP	https://www.reapdatabase.com
RG1.99	Regulatory Guide 1.99, Revision 2, "Radiation Embrittlement of Reactor Vessel Materials," U.S. Nuclear Regulatory Commission, May 1988, available at http://pbadupws.nrc.gov/docs/ML0037/ML003740284.pdf.
RG1.162	Regulatory Guide 1.162, "Format and Content of Report for Thermal Annealing of Reactor Pressure Vessels," USNRC, February 1996, ADAMS ML003740052.
Roberts 2000	G. K. Roberts, D. M. Chapman, S. L. Anderson, and J. D. Perock, "Palisades Reactor Pressure Vessel Neutron Fluence Evaluation," WCAP-15353, Revision 0 (January 2000).
Server 2010	William Server, et al. "For the Results on Attenuation of Neutron Embrittlement Effects in the Simulated RPV Wall," Journal of ASTM International, v7, n5. (2010)
Server 2017	William Server, et al. "The EPRI PWR Supplemental Surveillance Program (PSSP) Final Design and Implementation," Proceedings of the ASME 2017 Pressure Vessel and Piping Conference, July 16-20 2017, Waikoloa, Hawaii, U.S., PVP2017-65307.
Wichman 1998	K.R., Wichman, M.A. Mitchell, and A.L. Hiser, "Generic Letter 92-01 and RPV Integrity Assessment: Status, Schedule, and Issues," Presentation to NRC/Industry Workshop on RPV Integrity Issues, February 12, 1998, ADAMS ML110070570.

Appendix A

BASE METAL

	E185-82 Shift Categories		
	BASE-Low	**BASE-Medium**	**BASE-High**
E185-82 ΔT_{41J} Range [°C]	< 56	56 to 111	> 111
RG1.99 Predicted ΔT_{41J} at EOL[1] [°C]	29	84	140
RG1.99 Defined CF [°C]	**24.44**	**70.56**	**97.78**
Fluence at EOL (40 yrs) [n/cm^2]	3.6E+19	3.6E+19	3.6E+19
Product Form	BASE (PLATE)	BASE (PLATE)	BASE (PLATE)
Cu [wt%]	0.07	0.17	0.25
Ni [wt%]	0.6	0.6	0.6
Mn [wt%]	1.35	1.35	1.35
P [wt%]	0.01	0.01	0.01
Cold Leg Temp. [°C]	290	290	290
RG1.99 σ_Δ Value [°C]	9.4	9.4	9.4
Fluence for Capsule 1	6.0E+18	3.0E+18	1.5E+18
Fluence for Capsule 2	1.5E+19	6.0E+18	3E+18
Fluence for Capsule 3	3.6E+19	1.5E+19	6E+18
Fluence for Capsule 4	--	3.6E+19	1.5E+19
Fluence for Capsule 5	--	--	3.6E+19
Simulation Case ID (last # indicates number of capsules simulated	BASE-Low-2	BASE-Medium-2	BASE-High-2
	BASE-Low-3	BASE-Medium-3	BASE-High-3
		BASE-Medium-4	BASE-High-4
			BASE-High-5

[1] End of License, usually used to denote initial 40-year license as opposed to license renewal (LR) for first 20 year license extension and subsequent license renewal (SLR) for second 20 year license extension.

WELD METAL

	E185-82 Shift Categories		
	WELD-Low	**WELD-Medium**	**WELD-High**
E185-82 ΔT_{41J} Range [°C]	< 56	56 to 111	> 111
RG1.99 Predicted ΔT_{41J} at EOL [°C]	29	83	139
RG1.99 Defined CF [°C]	**22.78**	**62.36**	**107.78**
Fluence at EOL (40 yrs) [n/cm^2]	3.6E+19	3.6E+19	3.6E+19
Product Form	WELD	WELD	WELD
Cu [wt%]	0.03	0.17	0.3
Ni [wt%]	0.7	0.35	0.6
Mn [wt%]	1.5	1.5	1.5
P [wt%]	0.013	0.013	0.013
Cold Leg Temp. [°C]	290	290	290
RG1.99 σ_Δ Value [°C]	15.6	15.6	15.6
Fluence for Capsule 1	6.0E+18	3.0E+18	1.5E+18
Fluence for Capsule 2	1.5E+19	6.0E+18	3E+18
Fluence for Capsule 3	3.6E+19	1.5E+19	6E+18
Fluence for Capsule 4	--	3.6E+19	1.5E+19
Fluence for Capsule 5	--	--	3.6E+19
Simulation Case ID (last # indicates number of capsules simulated)	WELD-Low-2	WELD-Medium-2	WELD-High-2
	WELD-Low-3	WELD-Medium-3	WELD-High-3
		WELD-Medium-4	WELD-High-4
			WELD-High-5

Appendix B

Product Form	Country	Heat Identifier	# of ΔT_{41J} Values	Average Copper [wt%]	Average Nickel [wt%]	Average Temperature [°C]	Chemistry (Ratio) Adjustment Needed?	Temperature Adjustment Needed	CF_{TABLE} [°C]	CF_{FIT} [°C]	σ_{Δ} estimated from data [°C]	Scatter [°C]
FORGING	FRANCE	2569/3398	12	0.088	0.64	261	TRUE	TRUE	31.6	68.1	28.5	47.6
FORGING	U.S.	FMC201	8	0.154	0.78	292	FALSE	FALSE	65.4	45.3	6.5	14.4
FORGING	U.S.	FPI101	8	0.060	0.72	275	FALSE	FALSE	20.6	28.9	11.4	20.2
FORGING	U.S.	FPI201	8	0.077	0.70	275	FALSE	FALSE	27.2	32.9	8.9	17.0
FORGING	U.S.	FSQ201	8	0.130	0.74	285	FALSE	FALSE	52.5	49.7	6.7	12.7
FORGING	U.S.	FWB101	9	0.147	0.79	293	TRUE	FALSE	62.0	47.6	11.3	23.5
PLATE	S KOREA	NR82675-1	10	0.054	0.52	289	FALSE	FALSE	18.6	27.1	8.7	14.3
PLATE	S KOREA	NR82861-1	10	0.051	0.54	289	FALSE	FALSE	17.6	25.5	5.5	12.4
PLATE	U.S.	PBV101	8	0.200	0.54	285	FALSE	TRUE	78.8	83.1	14.3	22.1
PLATE	U.S.	PBV201	8	0.050	0.56	284	FALSE	FALSE	17.2	28.7	10.9	17.2
PLATE	U.S.	PCK101	8	0.140	0.49	281	FALSE	FALSE	52.8	52.5	4.8	8.9
PLATE	U.S.	PCL101	8	0.065	0.57	293	FALSE	TRUE	22.5	13.1	7.4	11.2
PLATE	U.S.	PDC201	8	0.140	0.66	283	FALSE	TRUE	56.4	55.5	4.2	8.6
PLATE	U.S.	PFA101	8	0.100	0.56	284	FALSE	FALSE	36.1	53.8	6.7	10.8
PLATE	U.S.	PFA201	12	0.195	0.60	284	FALSE	TRUE	80.6	79.9	6.7	12.4
PLATE	U.S.	PMC101	8	0.087	0.60	292	FALSE	TRUE	31.1	35.3	9.4	18.9
PLATE	U.S.	PZN101	8	0.110	0.49	276	FALSE	FALSE	40.5	44.2	6.8	12.3
PLATE	U.S.	PSA201	8	0.117	0.62	283	FALSE	TRUE	44.8	56.4	9.0	14.2
PLATE	U.S.	PST101	8	0.060	0.65	293	FALSE	TRUE	20.6	15.7	7.3	14.6
PLATE	U.S.	PST201	8	0.040	0.65	293	FALSE	FALSE	14.4	17.8	7.5	17.3
PLATE	U.S.	PVO201	10	0.051	0.58	292	FALSE	FALSE	17.4	15.6	11.5	20.6
PLATE	U.S.	PVO101	10	0.057	0.59	293	FALSE	FALSE	19.6	15.6	19.6	33.6
PLATE	U.S.	PVS101	10	0.100	0.51	291	FALSE	FALSE	36.1	24.3	10.9	19.8
PLATE	U.S.	PWC101	8	0.070	0.62	292	FALSE	TRUE	24.4	20.3	6.9	16.8
PLATE	TAIWAN	R4007-2	8	0.060	0.58	291	FALSE	FALSE	20.6	20.1	5.2	7.9
PLATE	TAIWAN	R5807-2	8	0.060	0.62	291	FALSE	FALSE	20.6	24.3	6.4	11.3
PLATE	S KOREA	R6008-2	10	0.060	0.65	290	FALSE	FALSE	20.6	24.3	10.9	19.0
PLATE	S KOREA	R6204-1	10	0.050	0.63	288	FALSE	FALSE	17.2	23.7	4.4	6.7
PLATE	S KOREA	R6309-2	10	0.050	0.66	290	FALSE	FALSE	17.2	17.7	5.2	10.7
PLATE	GERMANY	P10 BM 1	5	0.110	1.00	290	FALSE	FALSE	42.8	23.1	10.6	16.5
PLATE	GERMANY	P23 BM	7	0.100	0.83	282	FALSE	FALSE	37.2	44.0	7.6	11.6
SRM	U.S.	SASTM	26	0.200	0.18	283	FALSE	TRUE	55.6	52.4	9.9	19.7
SRM	U.S.	SHSS01	18	0.174	0.67	285	FALSE	TRUE	73.2	69.5	10.5	19.1
SRM	U.S.	SHSS02	65	0.170	0.64	283	FALSE	TRUE	71.1	63.8	16.3	37.3
WELD	S KOREA	42220/1512	8	0.041	0.60	286	TRUE	FALSE	31.1	26.6	6.8	13.8
WELD	S KOREA	4P7869	15	0.026	0.12	289	TRUE	TRUE	15.4	28.2	14.0	23.2
WELD	FRANCE	6322/1864	16	0.031	0.65	286	TRUE	FALSE	23.7	26.3	11.5	22.7
WELD	FRANCE	7774/1891	10	0.040	0.56	286	TRUE	FALSE	30.2	31.7	10.7	24.6
WELD	FRANCE	9730/1111	8	0.031	0.71	286	TRUE	FALSE	23.7	27.6	11.4	20.1
WELD	U.S.	WFA201	6	0.030	0.90	284	FALSE	TRUE	22.8	9.2	17.6	25.0
WELD	U.S.	WGIN01	6	0.240	0.52	287	FALSE	TRUE	89.7	86.4	6.6	9.9
WELD	GERMANY	P19 WM	5	0.230	1.08	284	FALSE	FALSE	137.1	114.4	3.5	5.3
WELD	GERMANY	P10 WM	5	0.070	0.93	290	FALSE	FALSE	52.8	23.7	2.6	4.2
WELD	GERMANY	P23 WM	5	0.190	1.15	282	FALSE	FALSE	129.7	67.0	2.9	5.0
WELD	GERMANY	P23 WM (man. Root)	6	0.100	0.44	282	FALSE	FALSE	56.7	20.8	4.6	8.0
WELD	U.S.	WML101	6	0.200	1.05	277	FALSE	TRUE	126.9	116.1	7.2	15.7
WELD	U.S.	13253	7	0.261	0.73	282	TRUE	TRUE	111.9	89.4	22.8	43.6
WELD	U.S.	61782	7	0.244	0.53	288	TRUE	TRUE	91.3	86.0	10.5	21.0
WELD	U.S.	72105	19	0.304	0.56	285	TRUE	TRUE	105.7	86.0	30.3	55.5
WELD	U.S.	72442	3	0.220	0.60	291	FALSE	FALSE	92.8	83.0	18.1	21.9
WELD	U.S.	72445	7	0.226	0.61	285	TRUE	TRUE	94.1	82.8	10.4	14.4
WELD	U.S.	90136	7	0.265	0.06	286	TRUE	TRUE	67.2	35.0	10.5	17.2
WELD	U.S.	305414	4	0.313	0.60	282	TRUE	TRUE	110.7	118.5	26.1	39.3
WELD	U.S.	442002	6	0.025	0.70	288	TRUE	FALSE	18.9	18.5	7.9	10.9
WELD	U.S.	895075	7	0.042	0.73	293	TRUE	TRUE	31.2	14.6	9.2	15.7
WELD	U.S.	1P3571	9	0.281	0.75	278	TRUE	TRUE	117.0	120.9	9.4	18.2
WELD	U.S.	34B009	6	0.200	1.05	277	FALSE	TRUE	126.9	116.1	7.2	15.7
WELD	U.S.	33A277	8	0.156	0.18	285	TRUE	TRUE	47.0	37.5	9.3	16.3
WELD	U.S.	406L44	14	0.287	0.59	289	TRUE	TRUE	104.6	97.4	14.1	21.9
WELD	U.S.	4P6052	6	0.029	0.07	292	TRUE	TRUE	14.5	9.1	10.5	14.2
WELD	U.S.	S3986	7	0.054	0.96	286	TRUE	TRUE	40.8	26.0	9.6	14.5
WELD	U.S.	W5214	7	0.234	0.90	284	TRUE	TRUE	122.7	123.6	13.7	23.6

Note: The light red shading denotes "sister plant" data (i.e., the same weld wire heat exposed to irradiation in more than one operating reactors).